

# MiR30-GALNT1/2 Axis-Mediated Glycosylation Contributes to the Increased Secretion of Inactive Human Prohormone for Brain Natriuretic Peptide (proBNP) From Failing Hearts

Yasuaki Nakagawa, MD, PhD; Toshio Nishikimi, MD, PhD; Koichiro Kuwahara, MD, PhD;\* Aoi Fujishima, BS; Shogo Oka, PhD; Takayoshi Tsutamoto, MD, PhD; Hideyuki Kinoshita, MD, PhD; Kazuhiro Nakao, MD; Kosai Cho, MD; Hideaki Inazumi, MD; Hiroyuki Okamoto, PhD; Motohiro Nishida, PhD; Takao Kato, MD, PhD; Hiroyuki Fukushima, MS; Jun K. Yamashita, MD, PhD; Wino J. Wijnen, PhD; Esther E. Creemers, PhD; Kenji Kangawa, PhD; Naoto Minamino, PhD; Kazuwa Nakao, MD, PhD; Takeshi Kimura, MD, PhD

**Background**—Recent studies have shown that plasma levels of the biologically inactive prohormone for brain natriuretic peptide (proBNP) are increased in patients with heart failure. This can contribute to a reduction in the effectiveness of circulating BNP and exacerbate heart failure progression. The precise mechanisms governing the increase in proBNP remain unclear, however.

**Methods and Results**—We used our recently developed, highly sensitive human proBNP assay system to investigate the mechanisms underlying the increase in plasma proBNP levels. We divided 53 consecutive patients hospitalized with heart failure into 2 groups based on their aortic plasma levels of immunoreactive BNP. Patients with higher levels exhibited more severe heart failure, a higher proportion of proBNP among the immunoreactive BNP forms secreted from failing hearts, and a weaker effect of BNP as estimated from the ratio of plasma cyclic guanosine monophosphate levels to log-transformed plasma BNP levels. Glycosylation at threonines 48 and 71 of human proBNP contributed to the increased secretion of proBNP by attenuating its processing, and GalNAc-transferase (GALNT) 1 and 2 mediated the glycosylation-regulated increase in cardiac human proBNP secretion. Cardiac GALNT1 and 2 expression was suppressed by microRNA (miR)-30, which is abundantly expressed in the myocardium of healthy hearts, but is suppressed in failing hearts.

**Conclusions**—We have elucidated a novel miR-30-GALNT1/2 axis whose dysregulation increases the proportion of inactive proBNP secreted by the heart and impairs the compensatory actions of BNP during the progression of heart failure. (*J Am Heart Assoc.* 2017;6:e003601. DOI: 10.1161/JAHA.116.003601.)

**Key Words:** microRNA • natriuretic peptide • signal transduction

Although originally isolated from the porcine brain, B-type or brain natriuretic peptide (BNP) is a cardiac hormone mainly produced and secreted by the ventricles.<sup>1,2</sup> Several pathological stimuli induce expression of a BNP precursor, preproBNP, in cardiac myocytes.<sup>3,4</sup> Removing the signal

peptide from preproBNP yields the BNP prohormone proBNP, which is in turn cleaved intracellularly to form the biologically active mature BNP (BNP-32) and inactive N-terminal proBNP (NT-proBNP) prior to their secretion (Figure 1A).<sup>4</sup> Plasma levels of both BNP and NT-proBNP are elevated in patients

From the Departments of Cardiovascular Medicine (Y.N., T.N., K. Kuwahara, A.F., H.K., Kazuhiro N., K.C., H.I., T. Kato, T. Kimura) and Primary Care and Emergency Medicine (K.C.), Department of Biology Chemistry, Human Health Sciences (S.O.), and Medical Innovation Center (Kazuwa N.), Kyoto University Graduate School of Medicine, Kyoto, Japan; Toyosato Hospital, Toyosato, Japan (T.T.); Diagnostics Division, Shionogi & Co., Ltd, Osaka, Japan (H.O.); Division of Cardiocirculatory Signaling, Okazaki Institute for Integrative Bioscience (National Institute for Physiological Sciences), National Institutes of Natural Sciences, Okazaki, Japan (M.N.); Department of Cell Growth and Differentiation, Center for iPS Cell Research and Application, Kyoto University, Kyoto, Japan (H.F., J.K.Y.); Department of Experimental Cardiology, Academic Medical Center, Amsterdam, The Netherlands (W.J.W., E.E.C.); National Cerebral and Cardiovascular Center Research Institute, Suita, Japan (K. Kangawa); Omics Research Center, National Cerebral and Cardiovascular Center, Suita, Japan (N.M.); Department of Cardiovascular Medicine, Shinshu University School of Medicine, Matsumoto, Japan (K. Kuwahara).

\*Dr Koichiro Kuwahara is currently located at Department of Cardiovascular Medicine, Shinshu University School of Medicine, 3-1-1 Asahi, Matsumoto, Nagano 390-8621, Japan. E-mail: kkuwah@shinshu-u.ac.jp

**Correspondence to:** Toshio Nishikimi, MD, PhD, and Koichiro Kuwahara, MD, PhD, Department of Cardiovascular Medicine, Kyoto University Graduate School of Medicine, 54 Kawahara-cho, Shogoin, Sakyo-ku, Kyoto 606-8507, Japan. E-mails: nishikim@kuhp.kyoto-u.ac.jp; kuwa@kuhp.kyoto-u.ac.jp

Received September 21, 2016; accepted December 22, 2016.

© 2017 The Authors. Published on behalf of the American Heart Association, Inc., by Wiley Blackwell. This is an open access article under the terms of the Creative Commons Attribution-NonCommercial License, which permits use, distribution and reproduction in any medium, provided the original work is properly cited and is not used for commercial purposes.

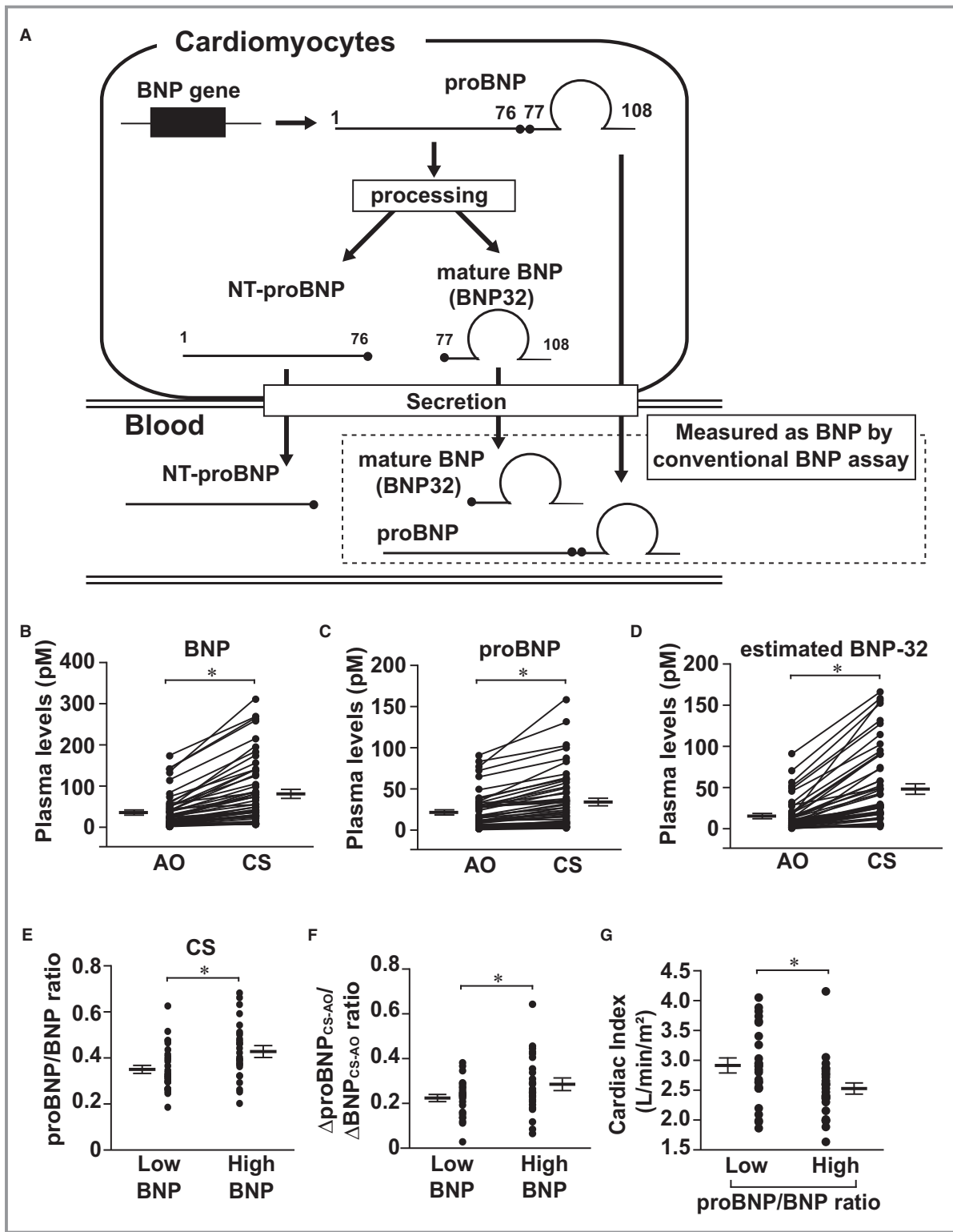


**Figure 1.** Cardiac secretion of prohormone for brain natriuretic peptide (proBNP) is increased in patients with heart failure. A, Schematic representation of proBNP processing and secretion by cardiac myocytes. Conventional BNP assays measure both human proBNP and mature BNP (dashed box). B through D, Plasma levels of BNP (B), proBNP (C), and estimated BNP-32 (D) in coronary sinus (CS) and aortic root (AO) of each individual (n=53). \**P*<0.05 using paired *t* test. E and F, proBNP/BNP ratios in the CS (E) and the  $\Delta\text{proBNP}_{\text{CS-AO}} / \Delta\text{BNP}_{\text{CS-AO}}$  ratio (F) in heart failure patients with high (n=27) or low BNP (n=26). \**P*<0.05 using unpaired *t* test. G, Cardiac index in heart failure patients with a high (n=27) or low proBNP/BNP ratio (n=26). Data are shown as dot plots with means±SEM. \**P*<0.05 using unpaired *t* test.

with cardiac hypertrophy or heart failure, and are currently established biomarkers whose levels correlate well with the prognosis and severity of heart failure.<sup>5,6</sup>

Recent studies have shown that unprocessed proBNP also circulates in healthy individuals, and that its plasma levels are elevated in patients with severe heart failure.<sup>7,8</sup> This is noteworthy because the immunoassay system currently used to measure human BNP levels detects both proBNP and mature BNP (Figure 1A).<sup>4,9</sup> Furthermore, recent in vitro studies have shown that proBNP has much less ability to stimulate cyclic guanosine monophosphate (cGMP) synthesis in vascular smooth muscle and endothelial cells than mature BNP.<sup>10</sup> Consequently, increases in the proportion of proBNP among the total secreted BNP forms, which include both proBNP and mature BNP, can lead to a reduction in the effectiveness of circulating BNP and the progression of heart failure. Indeed, the paradox in patients with severe heart failure is that the biological activity of BNP is attenuated, despite high circulating levels.<sup>11,12</sup> The mechanisms governing the cardiac secretion and peripheral metabolism of proBNP in heart failure patients have not been fully elucidated, however.

Within the Golgi apparatus of ventricular myocytes, human proBNP is post-translationally glycosylated to various degrees at 7 sites in its N-terminal region: threonine (Thr)36, serine (Ser)37, Ser44, Thr48, Ser53, Thr58, and Thr71.<sup>13</sup> The *O*-glycosylated proBNP is then transported to the trans-Golgi network, where it is cleaved into mature BNP and NT-proBNP, presumably by the proteolytic enzyme furin,<sup>9</sup> after which these products are secreted into the circulation. Recently, Semenov et al reported that *O*-glycosylation at Thr71 inhibits the processing of recombinant human proBNP in HEK293 cells.<sup>14</sup> On the other hand, Peng et al reported that wild-type (WT)-proBNP and a mutant proBNP in which Thr71 was substituted to alanine (Ala) were processed similarly in HL-1 cells.<sup>15</sup> Thus, the significance of *O*-glycosylation in the N-terminal region of human proBNP to its processing and secretion remained unclear. Importantly, most of the glycosylation sites on human proBNP are not conserved in rodent proBNP. In rats, nearly all circulating BNP is mature BNP-45, irrespective of the presence or absence of heart failure.<sup>16</sup>

In the present study, we used our recently developed, highly sensitive and selective assay system for human proBNP to investigate the cardiac production and peripheral metabolism of proBNP in patients with heart failure. Cardiac production of proBNP and the proportion of proBNP among secreted BNP forms are both increased in accordance with the severity of heart failure. We found that 2 *O*-glycosylation sites in human proBNP, Thr48 and Thr71, act cooperatively to inhibit the processing of proBNP, thereby increasing proBNP secretion by cardiac myocytes. Furthermore, we show that microRNA-30-mediated regulation of *N*-acetylgalactosaminyltransferase

(GalNac-T; GALNT) 1 and 2 expression modulates the glycosylation-regulated secretion of human proBNP from cardiac myocytes.

## Methods

### Blood Sampling

Blood was sampled from the coronary sinus (CS) and aortic root (AO) during cardiac catheterization in 53 consecutive patients hospitalized with heart failure at the Shiga University of Medical Science Hospital between 2003 and 2010 (study 1).<sup>11</sup> The patients' clinical characteristics are summarized in Table 1. We divided this study population into 2 groups based on median BNP level in the AO (high BNP group had BNP >22.3 pmol/L; low BNP group had BNP ≤22.3 pmol/L) to compare the proBNP/BNP ratios between these 2 groups. For the experiments measuring plasma proBNP and BNP levels in a peripheral vein and artery, venous blood was sampled from the superior vena cava or femoral vein and arterial blood was sampled from the cubital or femoral artery, respectively, of 25 consecutive patients hospitalized with heart failure at Kyoto University Hospital between 2011 and 2012 (study 2). The clinical characteristics of these patients are summarized in Table 2. Ethical approval was granted by the Kyoto University Hospital Ethical Committee and the Committee on Human Investigation at Shiga University of Medical Science. The aims of the study were explained to each participant, and written informed consent was obtained. All clinical investigations were conducted according to the principles expressed in the Declaration of Helsinki.

### Measurement of BNP and proBNP

We measured concentrations of both proBNP and BNP in plasma or conditioned medium using our recently developed, highly sensitive immunochemiluminescent assay for proBNP (Shionogi & Co. Ltd, Osaka, Japan) and the conventional immunochemiluminescent assay for BNP (Shionogi & Co. Ltd), respectively. In both assays, an antibody recognizing a common epitope in the C-terminal regions of proBNP and BNP was used as the capture antibody. An antibody recognizing an epitope in the N-terminal portion of proBNP was used as the signal antibody in the proBNP assay, while an antibody recognizing an epitope in the ring structure of BNP was used as the signal antibody in the conventional BNP assay. Importantly, because the affinities of the 2 signal antibodies were the same, we were able to accurately measure the proBNP/proBNP ratio in plasma or conditioned medium as an index of the proBNP processing efficiency. We previously addressed this issue in detail.<sup>7</sup> Both assays are specific for

**Table 1.** Clinical Characteristics and Plasma proBNP and BNP Levels in Heart Failure Patients With High or Low Aortic Plasma BNP Levels in Study 1

	Low BNP (n=27)	High BNP (n=26)	P Value
Age, y	60.0±2.3	69.5±1.8	0.0022
Height, cm	165.5±1.2	160.8±1.7	0.0279
Weight, kg	67.2±2.5	62.3±0.5	0.1542
Sex, M/F	24/3	21/5	0.4091
Etiology			
IHD/non IHD	17/10	14/12	0.5007
HR, beats/min	69.4±2.9	70.4±3.5	0.6724
SBP, mm Hg	124.1±4.4	132.1±3.9	0.6764
DBP, mm Hg	69.4±2.1	69.8±3.2	0.8178
MBP, mm Hg	88.9±2.6	95.6±3.1	0.7342
Serum creatinine, mg/dL	0.93±0.03	1.45±0.21	0.0734
Plasma cGMP, nmol/L	5.58±0.20	9.51±0.17	0.0008
Swan-Ganz data			
CO, L/min	5.3±0.2	4.0±0.2	0.0110
PCWP, mm Hg	8.2±0.8	13.9±1.6	0.0148
Mean PAP, mm Hg	13.4±0.9	21.2±2.0	0.0030
LVEF, %	44.6±2.6	37.2±1.2	0.2030
Ao level			
BNP, pmol/L	7.8±1.2	61.3±8.4	<0.0001
proBNP, pmol/L	4.7±0.8	36.2±4.4	<0.0001
Estimated BNP-32, pmol/L	3.1±0.5	25.1±4.4	<0.0001
CS level			
BNP, pmol/L	24.5±3.4	137.6±4.5	<0.0001
proBNP, pmol/L	8.8±1.4	57.2±6.7	<0.0001
Estimated BNP-32, pmol/L	15.8±2.1	80.4±9.0	<0.0001
CS—Ao level			
BNP, pmol/L	16.8±2.5	76.3±8.0	<0.0001
proBNP, pmol/L	4.1±0.8	21.0±3.2	<0.0001
Estimated BNP-32, pmol/L	12.7±1.8	55.3±6.2	<0.0001

Unpaired *t* test was used for the analysis. *P*<0.05 is considered significant. Ao indicates aortic root; BNP, brain natriuretic peptide; cGMP, cyclic guanosine monophosphate; CO, cardiac output; CS, coronary sinus; DBP, diastolic blood pressure; HR, heart rate; IHD, ischemic heart disease; LVEF, left ventricular ejection fraction; MBP, mean blood pressure; PAP, pulmonary artery pressure; PCWP, pulmonary capillary wedge pressure; proBNP, prohormone for brain natriuretic peptide; SBP, systolic blood pressure.

human BNP and proBNP, and do not cross-react to rat BNP-45 or rat proBNP-95. In this study, we use the term “BNP” to refer to immunoreactive BNP measured in the assay system using the same set of antibodies used in the conventional BNP assay system (Shionogi & Co., Ltd). Thus, immunoreactive BNP consists of both unprocessed proBNP and processed mature BNP. Estimated mature BNP was then calculated using the

**Table 2.** Clinical Characteristics of Patients With Heart Failure in Study 2

	n=25
Age, y	67.4±2.2
Height, cm	161.5±1.4
Weight, kg	60.7±2.1
Sex, M/F	16/9
Etiology	
IHD	8 (32.0%)
Valvular disease	6 (24.0%)
DCM	2 (8.0%)
HCM	4 (16.0%)
HHD	2 (8.0%)
Pulmonary hypertension	3 (12.0%)
HR, beats/min	71.3±3.3
SBP, mm Hg	121.1±3.2
DBP, mm Hg	68.1±2.9
PCWP, mm Hg	11.4±0.8
mPAP, mm Hg	19.0±1.0
eGFR, mL/min	47.8±4.3
Serum creatinine, g/dL	1.7±0.4
GOT, IU/L	23.6±2.7
GPT, IU/L	19.3±2.3

DBP indicates diastolic blood pressure; DCM, dilated cardiomyopathy; eGFR, estimated glomerular filtration rate; GOT, glutamate oxaloacetate transaminase; GPT, glutamate pyruvate transaminase; HCM, hypertrophic cardiomyopathy; HHD, hypertensive heart disease; HR, heart rate; IHD, ischemic heart disease; mPAP, mean pulmonary artery pressure; PCWP, pulmonary capillary wedge pressure; SBP, systolic blood pressure.

following formula: estimated mature BNP=BNP—proBNP. The transcardiac proBNP gradient ( $\Delta$ proBNP<sub>CS-AO</sub>) was calculated as proBNP in the CS minus proBNP in the AO.

### Animal Experiments

The animal care and all experimental protocols were reviewed and approved by the Animal Research Committee at Kyoto University Graduate School of Medicine and University of Amsterdam, and conformed to the US National Institute of Health Guide for the Care and Use of Laboratory Animals. Inbred male Dahl salt-sensitive (DS) rats (Japan SLC, Hamamatsu, Shizuoka, Japan) were fed a 0.3% NaCl (low salt: LS) diet until the age of 6 weeks, after which they were fed an 8% NaCl diet (high salt: HS).<sup>17,18</sup> As we reported previously, DS rats fed a high-salt diet (HS) developed hypertension and showed concentric left ventricular hypertrophy at 11 weeks of age.<sup>17,18</sup> At around 17 weeks of age, the DS rats fed a HS diet showed signs of congestive heart failure and showed decreased fractional shortening. DS rats fed a LS diet were

used as controls. For in vivo miR-30 inhibition we used 9-week-old C57BL/6J mice, injected subcutaneously with 5 mg/kg LNA based anti-miR-30c (Ribotask) or negative control anti-miR (Ribotask) at 2 different timepoints (day 0 and day 7). Mice were euthanized 4 weeks later, and hearts were snap-frozen in liquid nitrogen for protein analysis as previously reported.<sup>19</sup>

## Hemodynamics and Cardiac Echocardiography in DS Rats

Heart rate and blood pressure in DS rats were determined using the tail-cuff method with a noninvasive automated blood pressure apparatus (Softron BP-98A, Softron Co. Ltd, Tokyo, Japan) without anesthesia. Transthoracic echocardiography was performed as previously reported.<sup>17,20</sup> Prior to being euthanized at 15 to 17 weeks of age, rats were anesthetized briefly with inhaled diethyl ether (Wako Pure Chemical Industries, Osaka, Japan), and transthoracic echocardiography was performed using a Sonos-5500 echocardiograph (Agilent Technologies, Santa Clara, CA) equipped with a 15-MHz linear transducer. Intraventricular septal thickness, left ventricular dimension during diastole, and left ventricular dimension during systole were measured using M-mode echocardiography, and percent fractioning shortening was calculated.

## Tissue Sampling From DS Rats

To obtain heart tissues from DS rats for biochemical analyses, 17-week-old LS (n=17), and HS (n=14) rats were anesthetized with 3.0% of isoflurane and euthanized by decapitation without fasting. Hearts were rapidly snap-frozen in liquid nitrogen and stored at  $-80^{\circ}\text{C}$ .

## Cell Culture

Primary neonatal (2- to 4-day-old) rat ventricular myocytes (NRVMs) and cardiac fibroblasts were prepared on a Percoll gradient as described previously and plated in gelatin-coated 24-well dishes and incubated in Dulbecco's modified Eagle's medium supplemented with 10% FCS.<sup>3</sup>

A human induced pluripotent stem cell line (36B3) induced using episomal plasmid vectors encoding 6 factors (Oct3/4, Sox2, Klf4, L-Myc, LIN28, and Glis1) was established as previously reported.<sup>21</sup> Cardiomyocyte differentiation was induced using 836B3 as previously reported.<sup>22,23</sup> Derived cardiomyocytes were plated to a density of  $5 \times 10^4$  cells/well in gelatin-coated 24-well dishes for proBNP/BNP measurement, and at  $5 \times 10^5$  cells/dish in gelatin-coated 6-cm dishes for protein extract.

## Determination of Intracellular cGMP Accumulation and Plasma cGMP Levels

Cells in serum-free medium were preincubated for 1 hour in 0.1 mmol/L 3-isobutyl-1-methylxanthine and then treated for 10 minutes with 10 nmol/L human BNP, human glycosylated proBNP, or human nonglycosylated proBNP. The cells were then lysed in 0.1 mol/L HCl at room temperature for 20 minutes, after which the lysates were centrifuged at 600g, and the cGMP levels in the supernatant were measured using a radioimmunoassay kit (Yamasa Shoyu, Chiba, Japan). Plasma cGMP levels were determined in blood samples obtained from peripheral veins during cardiac catheterization in 53 consecutive patients hospitalized with heart failure at the Shiga University of Medical Science Hospital (study 1) by using the radioimmunoassay kit (Yamasa Shoyu).

## Plasmids

cDNA encoding full-length human pre-proBNP was amplified by polymerase chain reaction (PCR) using a human cDNA library as a template and cloned into pBluescript II SK(+) (Agilent Technologies, Santa Clara, CA). After confirming its sequence, cDNA encoding human pre-proBNP (WT) was introduced into pLV5IN-CVM Neo vector, which is a SIN-type lentiviral vector plasmid. Human proBNP is reportedly O-glycosylated at Thr36, Ser37, Ser44, Thr48, Ser53, Thr58, and Thr71 in its N-terminal region. To assess the function of the O-glycosylation of human proBNP, we generated the following set of human proBNP mutants in which various combinations of glycosylation sites were replaced with alanine: non-glyco, all 7 O-glycosylation sites were substituted with Ala; T71A, Thr71 was substituted to Ala; T48A, Thr48 was substituted with Ala; T48A/T71A, Thr48 and Thr71 were substituted with Ala; T58glyco, all O-glycosylation sites other than Thr58 were substituted with Ala; S53glyco, all O-glycosylation sites except Ser63 were substituted with Ala; T58glyco, all O-glycosylation sites except Thr58 were substituted with Ala; S53 glyco, all O-glycosylation sites except Ser53 were substituted with Ala; T48glyco, all O-glycosylation sites except Thr48 were substituted with Ala; S44glyco, all O-glycosylation sites except Ser44 were substituted with Ala; S37glyco, all O-glycosylation sites except Ser37 were substituted with Ala; T36glyco, all O-glycosylation sites except Thr36 were substituted with Ala; T48/T71glyco, the 5 O-glycosylation sites other than Thr48 and Thr 71 were substituted with Ala; S53/T71glyco, the 5 O-glycosylation sites other than Ser53 and Thr 71 were substituted with Ala. These mutants were constructed using QuikChange Lightning Site-Directed Mutagenesis Kits (Agilent Technologies) with human pre-proBNP gene cloned into pBluescript II as the template. The sequences of the constructs were verified by DNA



sequencing. The mutant genes were then introduced into pLV5IN-CMV Neo vector for lentivirus production.

GALNT1 3' untranslated region (UTR)-luc and GALNT2 3'UTR-luc were generated by inserting GALNT1 3'UTR or GALNT2 3'UTR containing miR-30 target sequences downstream of a gene encoding luciferase in the pMIR-REPORTER kit miRNA reporter expression vector (Thermo Fisher Scientific, Waltham, MA). The GALNT1 or -2 3'UTR was obtained by PCR using a human BAC clone as a template with the following primers: GALNT1 3'UTR, 5'- CCC TCA GAC TAG TGA CCA AAT TTA CAA AAA AAC G -3'(forward) and 5'- CAG CAC CAA GCT TCT GAA TCT GGT TCC AG -3'(reverse); GALNT-2 3'UTR, 5'- CTA TCA TAC TAG TGC AGG CCA GAG CAG -3' (forward) and 5'- CAT CAT CAA GCT TCG GCA CGC TTT GCT C -3' (reverse). Mutant GALNT1 3'UTR-luc and mutant GALNT2 3'UTR-luc, in which the miR-30 target sequences were mutated, were obtained through site-directed mutagenesis using GALNT1 3'UTR-luc or GALNT2 3'UTR-luc as the template with the following primers: GALNT 1 miR-30 mut, 5'- GAG ACT GTG CAC ACT GAT GAT ATC AAG ATT GAA AGA GTC TTT C -3'; GALNT 2 miR-30 mut, 5'-CTT TGC GGT GAG CTA TGA TAT CAT GAC ACA GTG TGC CAA AG -3'.

### Lentiviral Vector Production and Gene Transfer

HIV-based lentiviral vectors were generated using a Lenti-XTM HTX Ecotropic packaging system (Takara Bio Inc., Otsu, Japan) according to manufacturer's guidelines with WT and mutant human pre-proBNP gene contained in pLV5IN-CMV Neo vectors as mentioned above. NRVMs or cardiac fibroblasts were infected with each lentivirus for 24 hours after plating, after which the medium was exchanged. The culture medium was collected 96 hours after the infection.

### Gel Filtration Chromatography

Culture medium was extracted using Sep-Pak C18 cartridges (Waters, Milford, MA) as previously reported,<sup>7</sup> and the eluate was lyophilized and dissolved in 30% acetonitrile containing 0.1% TFA. The proteins in the solution were then separated using gel filtration high-performance liquid chromatography on a TSK gel G2000SWXL column (7.83300 mm; Tosoh Co., Tokyo, Japan), as previously reported.<sup>7</sup> The column effluent was fractionated every minute, and each fraction was analyzed using BNP and proBNP immunochemiluminescent assays as previously described.<sup>7</sup>

### Quantitative Real-Time-PCR Analysis

Using 50 ng of total RNA prepared from NRVMs or ventricles (apical halves of hearts) with Sepasol-RNA I (Nakarai, Tesque, Inc, Kyoto, Japan), levels of mRNA encoding rat GALNT1, 2, 3,

7, 10, 11, 12, and 15 were determined using quantitative real-time PCR according to the manufacturer's protocol (Applied Biosystems Inc, Foster City, CA). Relative mRNA levels were determined by normalization to the level of GAPDH mRNA. The relative mRNA levels in untreated WT samples were assigned a value of 1.0. Levels of miR-30a, b, c, d and e expression were determined using a Taqman MicroRNA RT kit, Taqman miRNA assay mix, and Taqman Universal PCR Master Mix II according to the manufacturer's protocol (Thermo Fisher Scientific). Relative miR-30 levels were determined by normalization to the level of U6. The relative miR-30 levels in the controls were assigned a value of 1.0. Taqman primers and probes for rat and mouse GALNTs, GAPDH, 18S, miR-30a, b, c, d, e and U6 were purchased from Applied Biosystems.

### Western Blot Analysis

Details of the methods used to prepare lysates from rat ventricles were described previously.<sup>3</sup> Briefly, samples were homogenized and sonicated in lysis buffer containing 20 mmol/L Tris-HCl (pH7.5), 150 mmol/L NaCl, 1 mmol/L Na<sub>2</sub>EDTA, 1 mmol/L EGTA, 1% Triton, 2.5 mmol/L sodium pyrophosphate, 1 mmol/L β-glycerophosphate, 1 mmol/L Na<sub>3</sub>VO<sub>4</sub>, 1 μg/mL leupeptin, and 1 mmol/L phenylmethylsulfonyl fluoride (Cell Signaling Technology, Inc, Danvers, MA). After the debris was cleared by centrifugation, the protein concentration in the supernatant was quantified as the crude extract. Extracts containing 50 μg of protein were separated by SDS-PAGE using 10% polyacrylamide gels and then analyzed by Western blotting using anti-GALNT1 (sc-68492; 1:1000; Santa Cruz Biotechnology Inc, Dallas, TX), anti-GALNT2 (#104070; 1:1000; GeneTex Inc, Irvine, CA), or anti-GAPDH (AB2302; 1:1000; Merck Millipore, Darmstadt, Germany) antibody.

### siRNA and miR-30c Mimic and Inhibitor

We purchased the following predesigned or designed siRNAs (Mission siRNA) from Sigma Aldrich (St. Louis, MO): siGALNT1 (SASI\_Rn01\_00031243), siGALNT2 (SASI\_Rn02\_00216578), siGALNT3 (SASI\_Rn01\_00120276), siGALNT7 (SASI\_Rn01\_00030444), siGALNT10 (SASI\_Rn01\_00054909), siGALNT11 (SASI\_Rn01\_00032481), siGALNT12 (SASI\_Rn02\_00317391), and GALNT15 (sense: CUG AUC AUC CAC GUU CUA UdTdT, antisense: AUA GAA CGU GGA UGA UCA GdTdT). The siRNAs were transfected into NRVMs using Lipofectamine RNAiMAX transfection reagent (Thermo Fisher Scientific) according to the manufacturer's instructions.

We purchased the following predesigned miR-30c mimic and inhibitor and their controls from GE Healthcare Bio-Sciences (Pittsburgh, PA): miRIDIAN microRNA rno-miR-30c-5p hairpin inhibitor (IH-320323-05), miRIDIAN microRNA rno-

miR-30c-5p mimic (C-320323-03), miRIDIAN microRNA Mimic Negative Control (CN-001000-01), and miRIDIAN microRNA Hairpin Inhibitor Negative Control (IN-001005-01).

## Statistical Analysis

Continuous variables are expressed as mean $\pm$ SE. The categorical data are summarized with percentages. Unpaired *t* tests were used for comparisons between 2 independent groups, while paired *t* tests were used for comparisons between 2 groups that were correlated. One-way ANOVA with post hoc Fisher's tests was used for comparisons among more than 2 groups and 2-way ANOVA with post hoc Fisher's tests was used for comparison among 4 or 6 groups containing 2 variables. Pearson's correlation coefficient (*r*) was used for the analysis of relationship between the proBNP/BNP ratios in veins and arteries of individual patients. Values of *P*<0.05 were considered significant.

## Results

### Increased Secretion of proBNP From Failing Hearts

To confirm that proBNP is secreted from failing hearts along with mature BNP, we measured proBNP and BNP levels in plasma collected from the AO and CS of 53 consecutive patients hospitalized with heart failure (study 1, Table 1). Measurements were made using both our newly developed human proBNP-specific immunoassay system and the conventional human BNP assay system, which detects both proBNP and mature BNP (Figure 1A).<sup>7</sup> We also estimated mature BNP levels by subtracting the values for proBNP from the total BNP. We found that levels of BNP, proBNP, and estimated mature BNP were all significantly higher in the CS than AO (Figure 1B through 1D). The average proBNP-to-BNP ratio (proBNP/BNP), which indicates the proportion of proBNP among immunoreactive BNP forms in the CS, was 0.39 $\pm$ 0.11 among the entire patient sample. When we divided our study population into 2 groups based on the median BNP level in the AO (high-BNP group, BNP >22.3 pmol/L; low-BNP group, BNP  $\leq$ 22.3 pmol/L), we found that the high-BNP group exhibited more severe heart failure than the low-BNP group (Table 1). In addition, levels of both proBNP and estimated mature BNP were significantly higher in the CS and AO in high-BNP group than the low-BNP group. The transcardiac gradient of proBNP ( $\Delta$ proBNP<sub>CS-AO</sub>), which is an index of cardiac proBNP secretion, was also significantly higher in high-BNP than low-BNP patients (Table 1), as were the proBNP/BNP ratio in the CS and the  $\Delta$ proBNP<sub>CS-AO</sub>/ $\Delta$ BNP<sub>CS-AO</sub> ratio (Figure 1E and 1F). These results indicate that proBNP is secreted from failing hearts, and the proportion of proBNP among the

secreted BNP forms increases with increases in the severity of heart failure.

Consistent with this finding, when we divided our study population into 2 groups based on the median proBNP/BNP ratio in the CS and evaluated the relationship between clinical parameters and the proBNP/BNP ratio, we found that the proBNP/BNP ratio correlates negatively with the cardiac index (Figure 1G).

### Peripheral Metabolism of proBNP and BNP in Heart Failure Patients

We next measured plasma proBNP and BNP levels in a peripheral vein and artery in 25 consecutive patients hospitalized with heart failure (study 2, Table 2). Venous BNP and estimated mature BNP levels were significantly lower than the arterial levels, but proBNP levels did not significantly differ between veins and arteries (Figure 2A through 2C). Furthermore, while the proBNP/BNP ratios in the veins correlated with the arterial ratios for the group (Figure 2D), within each individual the venous proBNP/BNP ratio was significantly higher than the arterial ratio (Figure 2E). This suggests proBNP has weaker affinity for its receptors and/or less susceptibility to degradation by peptidases (eg, neprilysin) than mature BNP in peripheral tissues. Indeed, the ability of glycosylated or nonglycosylated proBNP to stimulate cGMP production was much less than that of mature BNP in both cardiac myocytes and cardiac fibroblasts (Figure 2F and 2G). Consistent with these results, in 53 heart failure patients studied above (study 1), the venous plasma cGMP levels-to-logBNP<sub>AO</sub> ratios were significantly lower in the high-BNP group than the low-BNP group (Figure 2H).

### Two Glycosylation Sites, Thr48 and Thr71, Act Cooperatively to Attenuate proBNP Processing in Cardiac Myocytes

To further clarify the molecular mechanisms regulating human proBNP secretion from cardiac myocytes, we next infected cultured primary NRVMs with a lentivirus harboring human WT-proBNP gene and measured human proBNP and BNP secreted into the conditioned medium.<sup>7</sup> Although absolute values of BNP and proBNP levels varied (Figure 3A and 3B), proBNP/BNP ratios remained nearly constant across experiments (Figure 3C). Moreover, the proBNP/BNP ratio in medium conditioned by NRVMs expressing human proBNP (0.36 $\pm$ 0.03) was similar to the ratio in plasma samples from the CS of heart failure patients (0.39 $\pm$ 0.11) and in the medium conditioned by human iPS-derived cardiomyocytes (iPS-CMs) (0.38 $\pm$ 0.02) (Figure 3D). With iPS-CMs, although absolute values of BNP and proBNP levels varied (Figure 3E and 3F), proBNP/BNP ratios remained nearly constant across

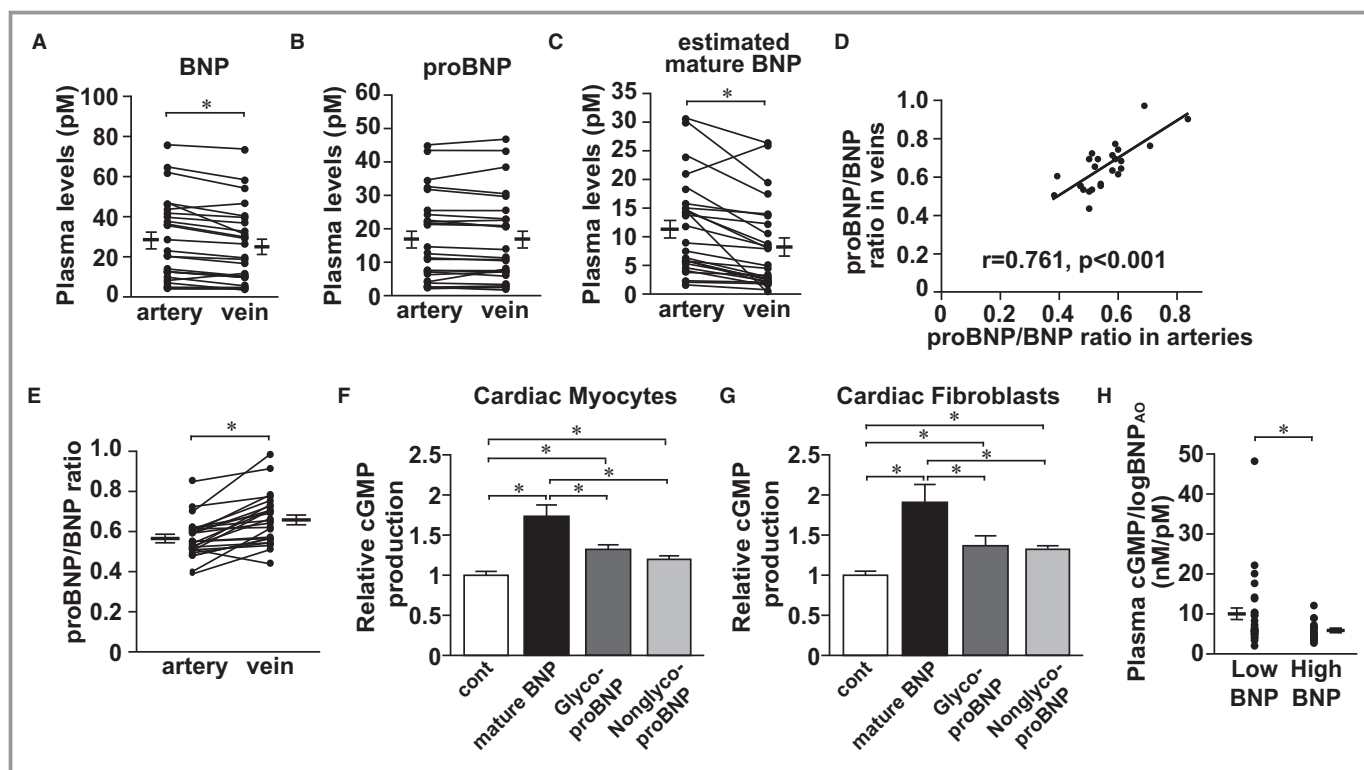


**Figure 2.** Peripheral metabolism of prohormone for brain natriuretic peptide (proBNP) in patients with heart failure. A through C, Dot plots with means±SEM showing plasma levels of BNP (A), proBNP (B), and estimated mature BNP (C) in a peripheral artery and vein in individual patients with heart failure (n=25). \*P<0.05 using paired *t* test. D, Relationship between the proBNP/BNP ratios in veins and arteries of individual patients. Pearson’s correlation coefficient (*r*) was used for the analysis. P<0.05 is considered significant. E, Dot plot with means±SEM showing proBNP/BNP ratios in a peripheral artery and vein in individual patients with heart failure (n=25). \*P<0.05 using paired *t* test. F and G, Relative levels of cyclic GMP (cGMP) in neonatal rat ventricular myocytes (NRVMs) (F) or cardiac fibroblasts (G) left untreated (control) or treated for 20 minutes with 10<sup>-8</sup> mol/L of mature BNP, glycosylated proBNP (Glyco-proBNP), or nonglycosylated proBNP (Nonglyco-proBNP) (n=8 each group). Relative cGMP levels in control NRVMs were assigned a value of 1.0. Data are shown as means±SEM. \*P<0.05 using 1-way ANOVA with post hoc Fisher’s test. H, Venous plasma cGMP levels-to-logBNP<sub>AO</sub> ratios (plasma cGMP/logBNP<sub>AO</sub>) in heart failure patients with high (n=27) or low BNP (n=26). Data are shown as dot plots with means±SEM. \*P<0.05 using unpaired *t* test.

experiments (Figure 3G), as was observed with NRVMs. These results indicate that NRVMs infected with a lentivirus harboring human proBNP recapitulate the production and secretion of proBNP and mature BNP by human cardiac myocytes.

We then sought to determine the impact of glycosylation in the N-terminal region of proBNP on its processing in ventricular myocytes. We infected NRVMs with lentiviruses harboring human WT-proBNP or 1 of several proBNP mutants in which 1 or more of the 7 glycosylated residues were replaced with alanine (Ala) (Figure 4A and 4B). In medium conditioned by NRVMs expressing the T71A mutant, in which Thr71 of proBNP was substituted with Ala, the proBNP/BNP ratio was significantly lower than in medium conditioned by NRVMs expressing WT-proBNP. The T71A proBNP mutant was thus cleaved into mature BNP to a significantly greater extent than WT-proBNP (Figure 5A). Furthermore, in medium from NRVMs expressing the non-glyco mutant, in which all 7 glycosylation sites of proBNP were replaced with Ala, the proBNP/BNP ratio was

markedly lower than in medium from cells expressing WT-proBNP, and even from cells expressing the T71A mutant (Figures 4B and 5A). This suggests that, in the absence of glycosylation, nearly all proBNP is cleaved to mature BNP and that glycosylation sites other than Thr71 are also involved in regulating proBNP processing in cardiac myocytes.

To identify the other glycosylation sites that affect proBNP processing, we measured human BNP and proBNP in medium conditioned by NRVMs expressing a human proBNP mutant in which only 1 of the glycosylation sites was preserved and the other 6 were replaced with Ala (T71glyco, T58glyco, S53glyco, T48glyco, S44glyco, S37glyco, and T36glyco) (Figures 4B and 5B). As anticipated, the proBNP/BNP ratio was significantly higher in medium conditioned by NRVMs expressing T71glyco than by NRVMs expressing the non-glyco mutant. Among the other mutants tested, the proBNP/BNP ratio in medium conditioned only by NRVMs expressing T48glyco was significantly higher than that conditioned by NRVMs expressing the non-glyco mutant (Figure 5B). These results indicate that 2



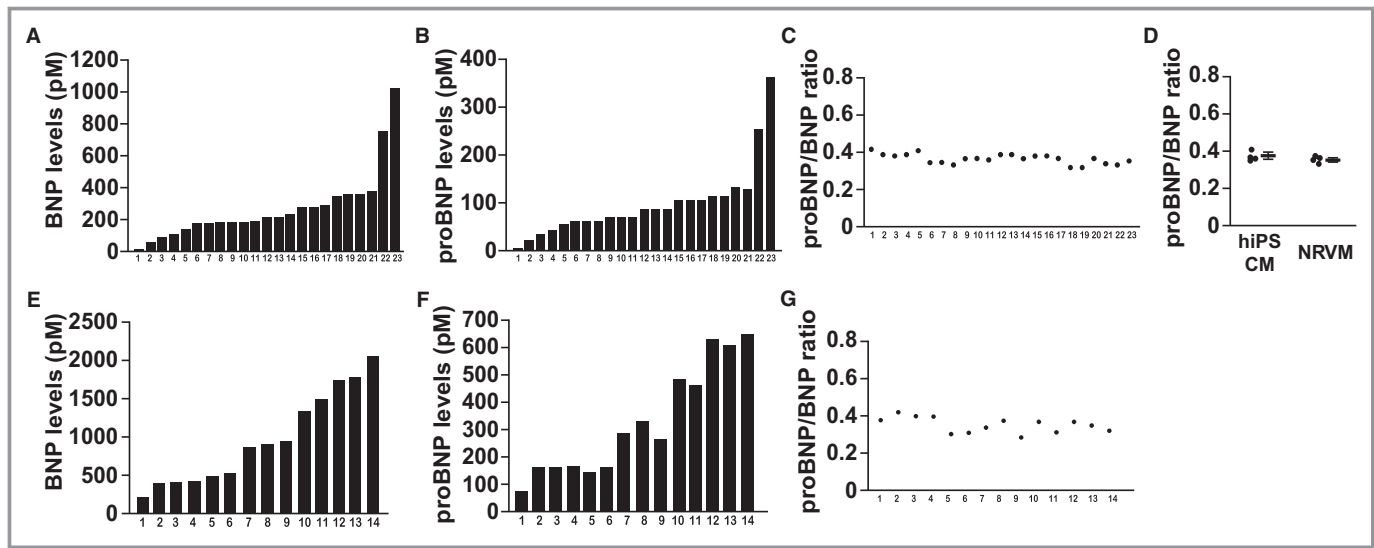


**Figure 3.** Prohormone for brain natriuretic peptide (proBNP)/BNP ratios in conditioned medium of neonatal rat ventricular myocytes (NRVMs) expressing human proBNP and human iPS-derived cardiac myocytes (iPS-CM). A through C, BNP levels (A), proBNP levels (B), and proBNP/BNP ratios (C) in medium conditioned by NRVMs expressing human wild-type proBNP (WT-proBNP) in each experiment (n=23). D, ProBNP/BNP ratios in medium conditioned by human iPS-derived cardiomyocytes (hiPS CM) and NRVMs. Data are shown as dot plots with means±SEM (n=4 each). E through G, BNP levels (E), proBNP levels (F), and proBNP/BNP ratios (G) in medium conditioned by human iPS-CM in each experiment (n=14).

glycosylation sites, Thr71 and Thr48, are important for the processing of proBNP in ventricular myocytes. We further found that the proBNP/BNP ratio in medium conditioned by NRVMs expressing T48/T71glyco was significantly higher than in medium conditioned by NRVMs expressing either T48glyco or T71glyco alone, though the ratio was still lower than in medium conditioned by NRVMs expressing WT-proBNP (Figures 4B and 5C). The S53/T71glyco mutant showed no additive effects on the proBNP/BNP ratio in medium conditioned by NRVMs expressing T71glyco (Figure 5C). Conversely, the proBNP/BNP ratio in medium conditioned by NRVMs expressing either the T71A or T48A mutant was significantly lower than in medium conditioned by NRVMs expressing WT-proBNP (Figure 5D). Furthermore, the proBNP/BNP ratio in medium conditioned by NRVMs expressing the T48A/T71A mutant was markedly lower than in medium conditioned by NRVMs expressing either the T71A or T48A mutant and was nearly identical to the ratio in medium conditioned by NRVMs expressing the non-glyco mutant (Figure 5D). Apparently glycosylation of both Thr71 and Thr48 is necessary to fully inhibit cleavage of proBNP. These results demonstrate that Thr48 and Thr71 act cooperatively to play an essential role in the processing and secretion of human proBNP in cardiac myocytes.

As with cardiac myocytes, the proBNP/BNP ratio was significantly lower in medium conditioned by cardiac fibroblasts expressing either the T71A or T48A mutant than WT-proBNP (Figure 5E). Thus, the machinery involved in the glycosylation-dependent regulation of proBNP processing is conserved, at least in part, between cardiac ventricular

myocytes and fibroblasts. This is consistent with our earlier finding that the ubiquitously expressed proteolytic enzyme furin contributes to the processing of proBNP.<sup>16</sup>

To further confirm that Thr48 and Thr71 are glycosylated in proBNP, we used gel-filtration in combination with an immunochemiluminescent technique to compare the molecular sizes of proBNP and mature BNP in medium conditioned by NRVMs expressing WT-proBNP or the T71A, T71 glyco or non-glyco mutant.<sup>7</sup> The peak proBNP immunoreactivity in medium conditioned by NRVMs expressing T71A was shifted slightly rightward as compared to the WT-proBNP peak (Figure 6A and 6B), which means T71A is smaller in size. In addition, the amplitude of the proBNP immunoreactivity peak relative to the mature BNP peak in medium conditioned by NRVMs expressing T71A is markedly smaller than in medium conditioned by NRVMs expressing WT-proBNP, which is consistent with T71A being more easily cleaved to form mature BNP than WT-proBNP (Figure 6A and 6B). In addition, the proBNP immunoreactivity peaks for T71glyco and non-glyco were shifted farther rightward than those for T71A and WT-proBNP, as would be expected (Figure 6A through 6E). Essentially the same results were obtained for comparisons among WT-proBNP and the T48A, T48glyco, and non-glyco mutants (Figure 6F through 6J).

### GALNT1/2 Impair the Processing of proBNP in Cardiac Myocytes

The *N*-acetylgalactosamine (GalNAc)-transferase (GALNT) family catalyzes the first step in the biosynthesis forming

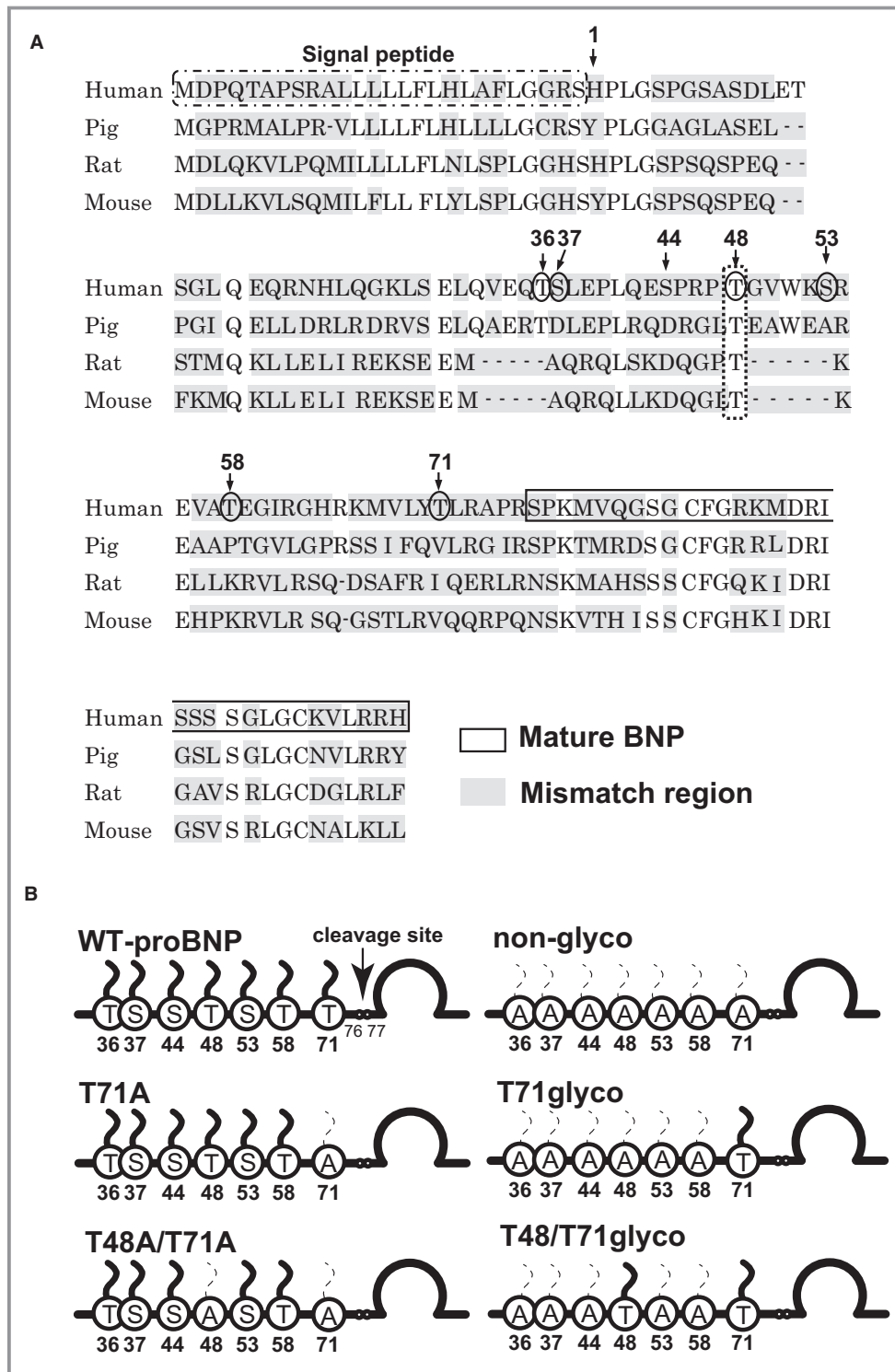


**Figure 4.** Mutation in glycosylation sites in the N-terminal region of prohormone for brain natriuretic peptide (proBNP). A, Comparison of the amino acid sequences of pre-proBNP from human, pig, rat, and mouse. Amino acids with a solid line circle are potentially glycosylated residues in human proBNP. Note that Thr48 is conserved among the 4 species (dashed line circle). B, Schema for wild-type (WT)-proBNP and various proBNP mutants used in this study. T71A: mutant in which threonine (Thr) 71 is substituted with alanine (Ala). T48A/T71A: mutant in which Thr71 and Thr48 are substituted with Ala. Non-glyco: mutant in which all 7 glycosylation sites are substituted with Ala. T71-glyco: mutant in which all glycosylation sites except Thr71 are substituted with Ala. T48/T71-glyco: mutant in which the 5 glycosylation sites other than Thr71 and Thr48 are substituted to Ala.

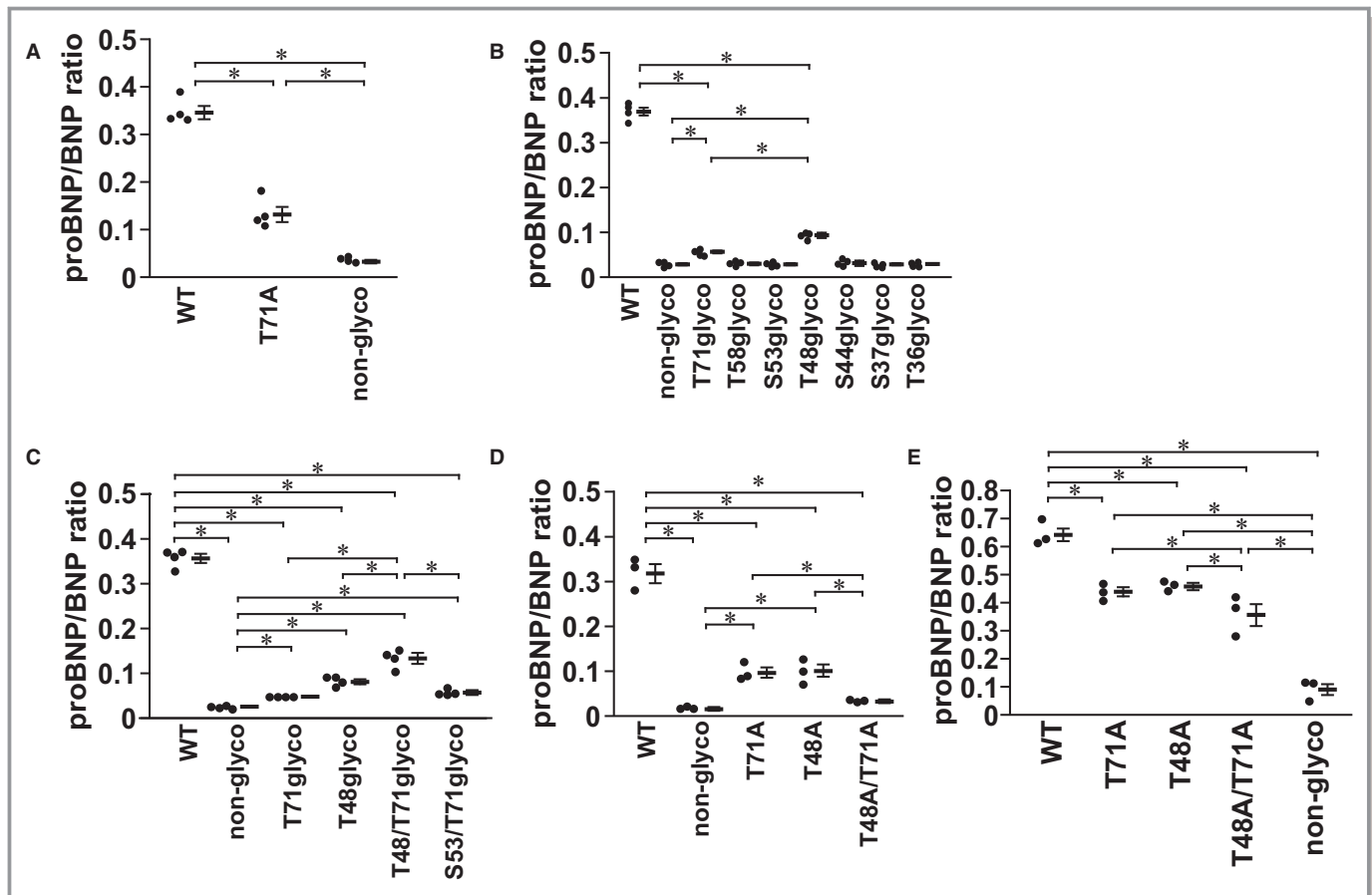


**Figure 5.** Two glycosylation sites, Thr48 and Thr71, modulate the processing of prohormone for brain natriuretic peptide (proBNP) in cardiac myocytes. A through D, ProBNP/BNP ratios in medium conditioned by neonatal rat ventricular myocytes expressing WT-proBNP or the indicated proBNP mutants. Data are shown as dot plots with means±SEM (n=4 each in A through C; n=3 in D). \*P<0.05 using 1-way ANOVA with post hoc Fisher’s test. E, ProBNP/BNP ratios in medium conditioned by cardiac fibroblasts expressing wild-type (WT)-proBNP or indicated proBNP mutants. Data are shown as dot plots with means±SEM. \*P<0.05 (n=3 each) using 1-way ANOVA with post hoc Fisher’s test. Non-glyco: mutant proBNP in which all 7 glycosylation sites are substituted with alanine (Ala). T71-glyco: mutant proBNP in which all glycosylation sites except threonine (Thr) 71 are substituted with Ala. T58-glyco: mutant proBNP in which all glycosylation sites except Thr58 are substituted with Ala. S53-glyco: mutant proBNP in which all glycosylation sites except serine (Ser) 53 are substituted with Ala. T48-glyco: mutant proBNP in which all glycosylation sites except Thr48 are substituted with Ala. S44-glyco: mutant proBNP in which all glycosylation sites except Ser44 are substituted with Ala. S37-glyco: mutant proBNP in which all glycosylation sites except Ser37 are substituted with Ala. T36-glyco: mutant proBNP in which all glycosylation sites except Thr36 are substituted with Ala. T48/T71-glyco: mutant proBNP in which the 5 glycosylation sites other than Thr71 and Thr48 are substituted with Ala. S53/T71-glyco: mutant proBNP in which the 5 glycosylation sites other than Thr71 and Ser53 are substituted to Ala. T71A: mutant proBNP in which Thr71 is substituted with Ala. T48A: mutant proBNP in which in which Thr48 is substituted with Ala. T48A/T71A: mutant proBNP in which Thr71 and Thr48 are substituted with Ala.

the GalNAcα1-O-Ser/Thr linkage in O-glycosylation. To determine which GALNTs are involved in the O-linked glycosylation of proBNP in cardiac myocytes, we evaluated the effect of knocking down each of the GALNTs reportedly expressed in the heart (GALNT 1, 2, 7, 10, 11, 12, and 15) using the corresponding siRNA<sup>24</sup> (Figure 7A). Among these, only knockdown of GALNT1 or 2 significantly reduced the proBNP/BNP ratio in medium conditioned by NRVMs expressing WT-proBNP (Figure 7B). Knockdown of GALNT3 did not affect the proBNP/BNP ratio in medium conditioned by NRVMs expressing WT-proBNP (Figure 7C and 7D). Furthermore, in medium

conditioned by NRVMs expressing T48A/T71A, knockdown of GALNT1 or 2 did not affect the proBNP/BNP ratio (Figure 7E).

We hypothesized that a decrease in the processing efficiency of proBNP accounts for the increased proportion of proBNP secreted by failing ventricles. To test that idea, we assessed the effect of hypertrophic stimuli on proBNP processing efficiency. We evaluated proBNP and BNP levels in medium conditioned by FCS- or endothelin-1 (ET-1)-treated NRVMs expressing WT-proBNP or a non-glyco mutant (Tables 3 and 4), and then calculated the proBNP/BNP ratio. FCS dose-dependently increased the proBNP/BNP ratio in

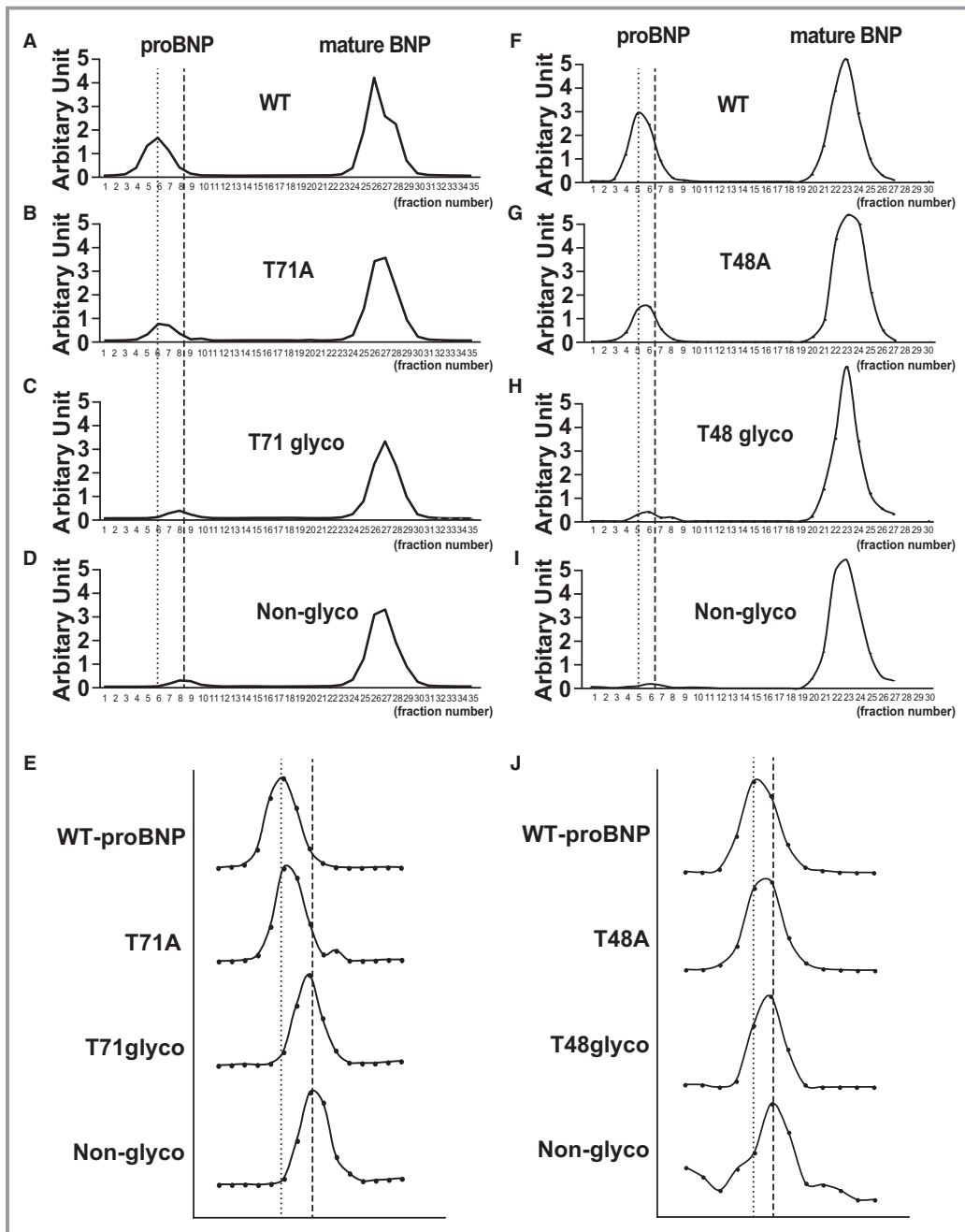


**Figure 6.** Gel filtration analysis reveals glycosylation of human pro brain natriuretic peptide (proBNP). A through J, Molecular sizes of human proBNP in medium conditioned by neonatal rat ventricular myocytes (NRVMs) expressing wild-type (WT)-proBNP or the indicated proBNP mutants were determined by gel filtration analysis. A through D, Molecular sizes of human proBNP and mature BNP in medium conditioned by NRVMs expressing WT-proBNP and T71A, T71glyco, or non-glyco mutant. E, Enlarged view of the peak proBNP immunoreactivity in medium conditioned by NRVMs expressing WT-proBNP and T71A, T71glyco, or non-glyco mutant. F through I, Molecular sizes of human proBNP and mature BNP in medium conditioned by NRVMs expressing WT-proBNP, and T48A, T48glyco, or non-glyco mutant. J, Enlarged view of the peak proBNP immunoreactivity in medium conditioned by NRVMs expressing WT-proBNP and T48A, T48glyco, or non-glyco mutant. Fractions were assayed using the conventional BNP assay system. The first peak shows proBNP, and the second shows mature BNP. Dotted lines and dashed lines indicate the immunoreactivity peaks for WT-proBNP and non-glyco mutant proBNP, respectively. Non-glyco: mutant proBNP in which all 7 glycosylation sites are substituted with alanine (Ala). T71-glyco: mutant proBNP in which all glycosylation sites except threonine (Thr) 71 are substituted with Ala. T48-glyco: mutant proBNP in which all glycosylation sites except Thr48 are substituted with Ala. T48A: mutant proBNP in which Thr48 is substituted with Ala. T71A: mutant proBNP in which Thr71 is substituted with Ala. T48A: mutant proBNP in which Thr48 is substituted with Ala.



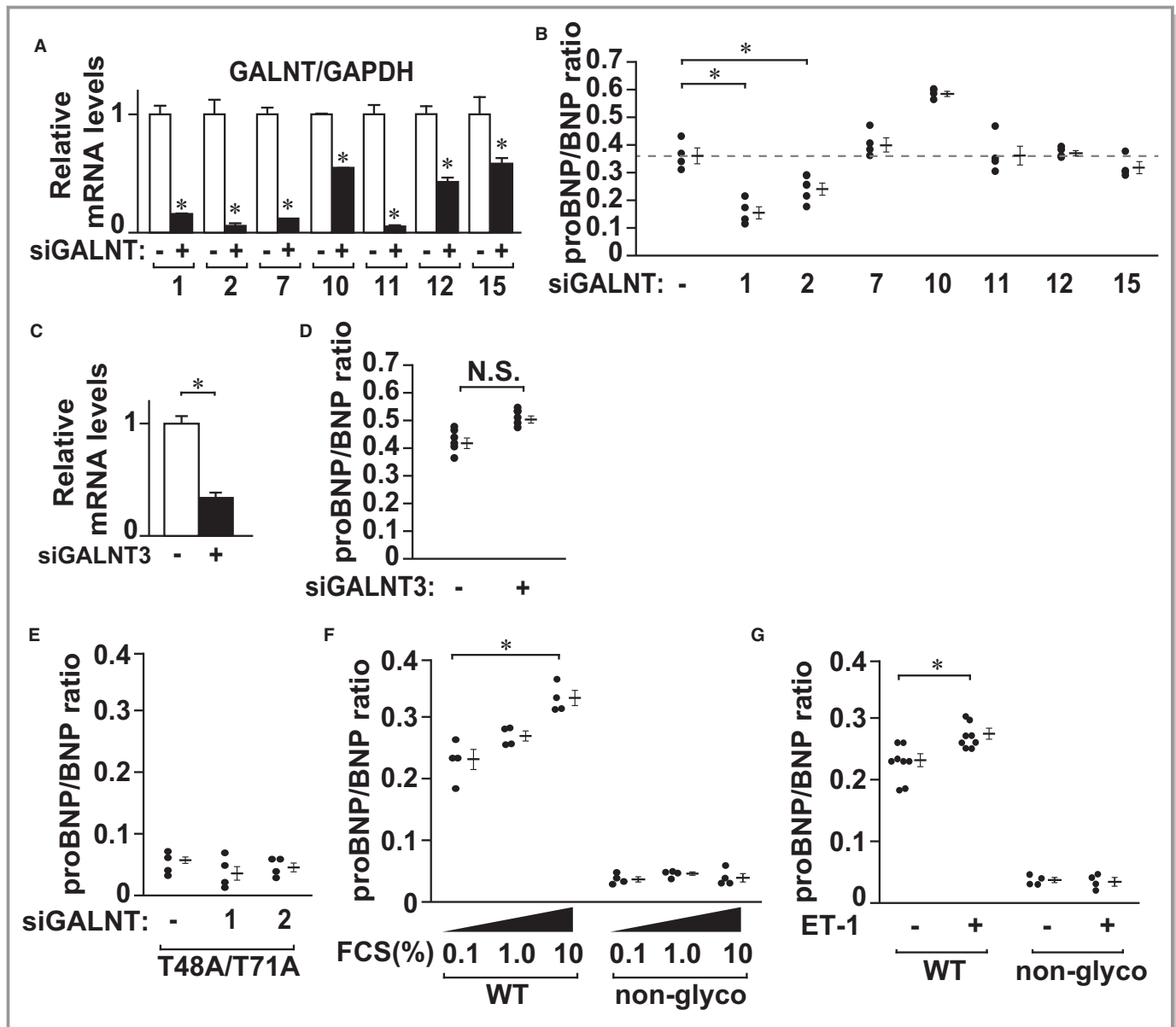


**Figure 7.** GALNT1 and 2 suppress prohormone for brain natriuretic peptide (proBNP) processing in cardiac myocytes. A, mRNA expression of indicated *N*-acetylglucosaminyltransferase (GALNT) genes in neonatal rat ventricular myocytes (NRVMs) transfected with the corresponding siRNAs. The mRNA levels in NRVMs with control oligo were assigned a value of 1.0 (n=3 in each group). Data are shown as means±SEM. \*P<0.05 vs control, using unpaired *t* tests. B, proBNP/BNP ratios in medium conditioned by NRVMs expressing WT-proBNP and transfected with siRNA targeting the corresponding GALNT (n=4 each). \*P<0.05 using 1-way ANOVA with post hoc Fisher's test. C, mRNA expression of GALNT3 gene in NRVMs transfected with the siRNA for GALNT3. GALNT3 mRNA levels in NRVMs with control oligo were assigned a value of 1.0 (n=3 in each group). Data are shown as means±SEM. \*P<0.05 vs control, using unpaired *t* tests. D, proBNP/BNP ratios in medium conditioned by NRVMs expressing WT-proBNP and transfected with siRNA targeting GALNT3 (n=4 each). N.S.: not significant using 1-way ANOVA with post hoc Fisher's test. E, proBNP/BNP ratios in medium conditioned by NRVMs expressing T48A/T71A mutant and transfected with GALNT1 or 2 siRNA (n=4 each). T48A/T71A mutant: mutant proBNP in which Thr71 and Thr48 are substituted with Ala. F and G, proBNP/BNP ratios in medium conditioned by NRVMs expressing WT-proBNP or non-glyco and stimulated with the indicated concentrations of fetal calf serum (FCS) (n=4 each) (F) or  $5 \times 10^{-8}$  mol/L of endothelin-1 (ET-1) (n=8 each in WT-proBNP and 4 each in non-glyco) (G). \*P<0.05 using 2-way ANOVA with post hoc Fisher's test. In E–G, data are shown as dot plots with means±SEM. H and I, GALNT1/2 expression in NRVMs treated with 10% FCS. Representative Western blots (H) and relative protein levels (I) are shown. Data are the means±SEM. The relative protein levels in untreated NRVMs (control) were assigned as 1.0. \*P<0.05 vs control, using unpaired *t* test (n=6 each).

medium conditioned by NRVMs expressing WT-proBNP, but had no effect on the ratios in medium conditioned by NRVMs expressing the non-glyco mutant (Figure 7F and Table 3). ET-

1, which is well known to induce hypertrophic responses, had a similar effect (Figure 7G and Table 4). These results strongly suggest that pathological hypertrophic signaling-

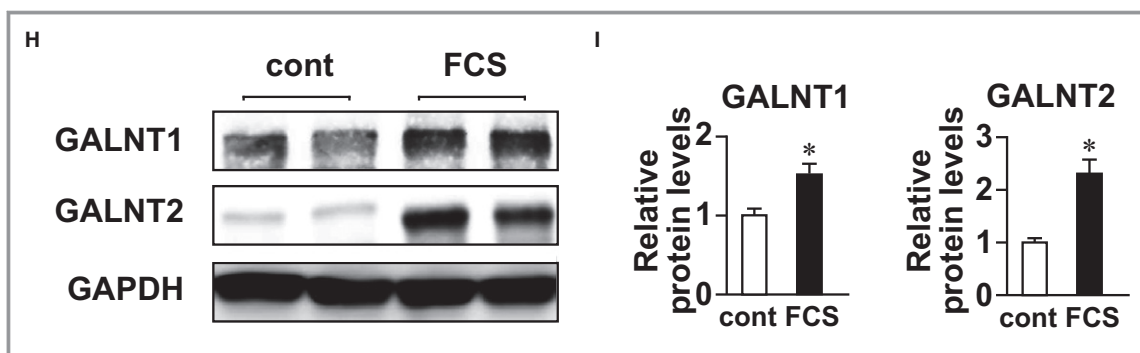


Figure 7. Continued

induced alterations in the glycosylation status of the proBNP N-terminal region are responsible for the increased proportion of proBNP secretion by failing hearts. Consistent with this finding, FCS significantly increased the levels of GALNT1/2 proteins in NRVMs (Figure 7H and 7I).

### The microRNA-30 Family Promotes proBNP Processing by Suppressing GALNT1/2 Expression in Cardiac Myocytes

We next sought to address the molecular mechanism by which GALNT1/2 expression is increased in response to hypertrophic stimulation. Expression levels of GALNT1/2 mRNA in NRVMs were significantly increased by fetal calf serum, but the increase in their transcript levels appears somewhat modest compared to the increase in their protein levels (Figure 8A). We identified a conserved target site for miR-30 family members (miR-30a, b, c, d, and e) in the 3'-untranslated region (UTR) of both the GALNT1 and GALNT2

genes (Figure 8B). Although they are ubiquitously expressed, miR-30s are among the most strongly expressed microRNAs in cardiac myocytes.<sup>25</sup> However, miR-30 expression in NRVMs was significantly reduced by FCS (Figure 8C). Overexpression of a miR-30c mimic significantly reduced endogenous levels of GALNT1 and GALNT2 protein (Figure 9A and 9B), whereas overexpression of a miR-30 inhibitor increased their protein levels in NRVMs (Figure 9C and 9D). The miR-30c mimic also significantly reduced the activity of a luciferase reporter linked to the 3'-UTR of GALNT1/2, and a mutation in the predicted miR-30 target site in the 3'-UTR prevented that repression (Figure 9E and 9F). All of these results indicate that reduced expression of miR-30 family members caused by FCS led to increases in GALNT1/2 expression in NRVMs. Furthermore, the miR-30c mimic significantly reduced the proBNP/BNP ratio in medium conditioned by NRVMs expressing WT-proBNP (Figure 9G). As was observed with NRVMs expressing WT-proBNP, FCS dose-dependently increased the proBNP/BNP ratio in medium conditioned by human iPS-CM (Figure 10A). In human iPS-CMs, GALNT1 or GALNT2 knockdown

**Table 3.** ProBNP, BNP, and proBNP/BNP Ratio in Medium Conditioned by FCS-Treated NRVMs Expressing WT-proBNP or Non-Glyco Mutant

	FCS 0.1%	FCS 1%	FCS 10%
<b>WT-proBNP</b>			
BNP, pmol/L	184.2±4.2	289.2±6.5	360.3±3.7
proBNP, pmol/L	43.9±2.9	79.5±2.5	122.9±3.5
proBNP/BNP	0.237±0.01	0.275±0.0	0.341±0.0
<b>Non-glyco</b>			
BNP, pmol/L	264.9±9.6	123.4±19.4	185.0±29.8
proBNP, pmol/L	9.9±1.6	3.4±0.72	7.9±1.8
proBNP/BNP	0.037±0.0	0.027±0.0	0.040±0.0

BNP indicates brain natriuretic peptide; FCS, fetal calf serum; non-glyco, non-glyco mutant of proBNP; NRVMs, neonatal rat ventricular myocytes; proBNP, prohormone for brain natriuretic peptide; WT-proBNP, wild-type proBNP.

**Table 4.** ProBNP, BNP, and proBNP/BNP Ratio in Medium Conditioned by ET-1-Treated NRVMs Expressing WT-proBNP or Non-Glyco Mutant

	ET(-)	ET(+)
<b>WT-proBNP</b>		
BNP, pmol/L	184.2±3.9	222.5±15.2
proBNP, pmol/L	43.9±2.7	63.0±5.4
proBNP/BNP	0.239±0.01	0.281±0.01
<b>Non-glyco</b>		
BNP, pmol/L	157.5±20.9	120.6±24.2
proBNP, pmol/L	5.7±0.9	4.25±0.6
proBNP/BNP	0.038±0.04	0.035±0.01

BNP indicates brain natriuretic peptide; ET-1, endothelin-1; non-glyco, non-glyco mutant of proBNP; NRVMs, neonatal rat ventricular myocytes; proBNP, prohormone for brain natriuretic peptide; WT-proBNP, wild-type proBNP.

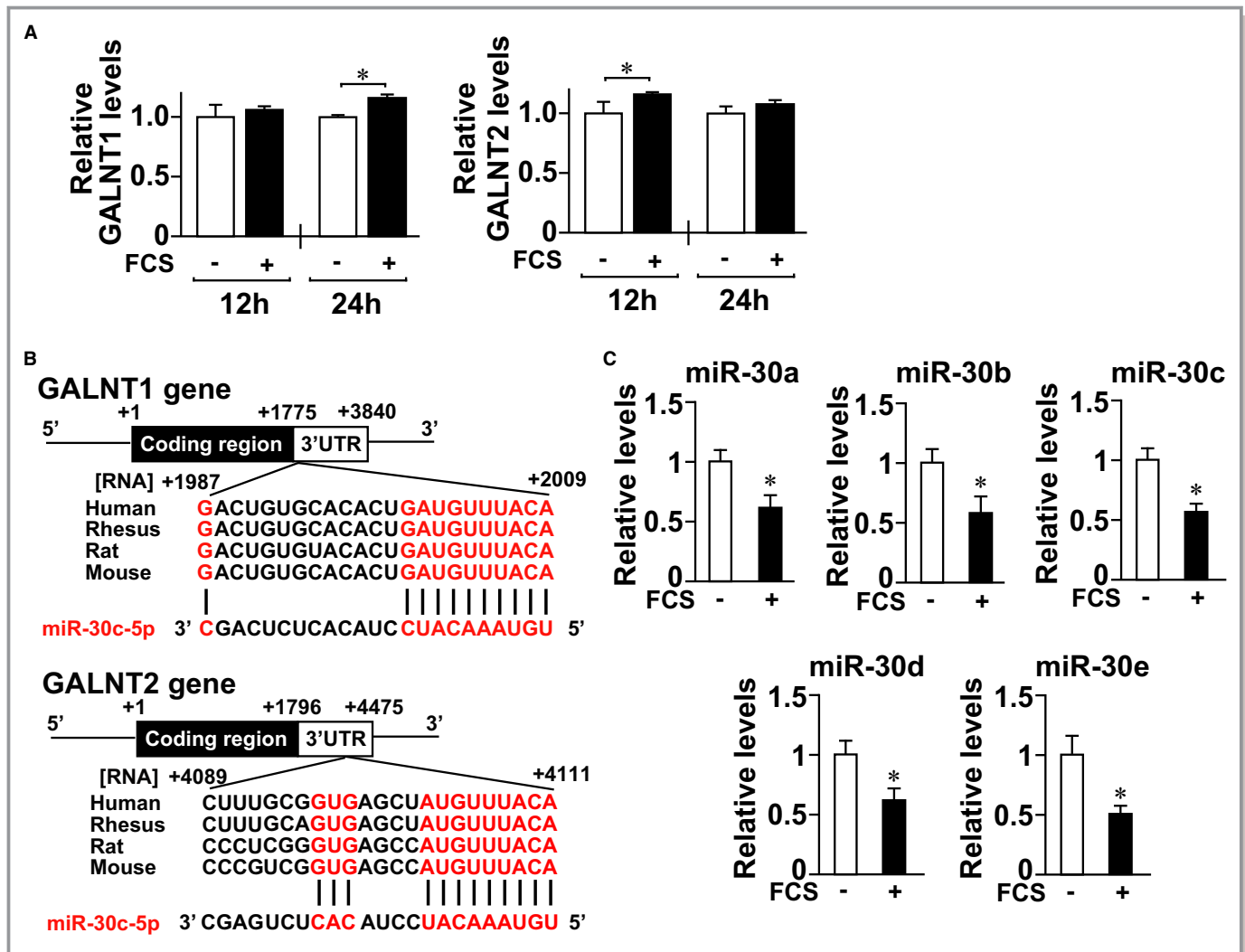


**Figure 8.** A conserved target site for miR-30 family members in the 3'-untranslated region (UTR) of both the GALNT1 and GALNT2 genes. A, Relative expression levels of GALNT1 and 2 mRNA in neonatal rat ventricular myocytes (NRVMs) treated with 10% fetal calf serum (FCS) for the indicated times. Relative mRNA levels were determined by normalization to the level of GAPDH mRNA. Data are shown as means±SEM. The relative mRNA levels in untreated NRVMs were assigned a value of 1.0. \**P*<0.05 using unpaired *t* tests. B, Schema of the GALNT1/2 genes. 3'UTR: 3' untranslated region. C, Quantitative real-time polymerase chain reaction analysis of the miR-30 family in NRVMs with 10% FCS stimulation (n=12 each). \**P*<0.05 vs NRVMs without FCS, using unpaired *t* test.

significantly reduced the proBNP/BNP ratio in their conditioned medium (Figure 10B and 10C). Moreover, overexpression of the miR-30c mimic in iPSC-CMs significantly reduced GALNT1/2 levels (Figure 10D and 10E) and the proBNP/BNP ratio in the conditioned medium (Figure 10F).

In vivo administration of the miR-30c inhibitor to mice significantly increased cardiac levels of GALNT1/2 (Figure 10G and 10H). In addition, miR-30 expression was significantly lower and GALNT1/2 levels were significantly higher in the failing hearts of DS rats fed a HS diet than in the control hearts of DS rats fed a LS diet (Figure 11A through 11C and Tables 5, 6).<sup>18</sup>

These results support our findings that decreased expression of miR-30s contributes to the increase in GALNT1 and 2

expression in failing hearts, which reduces the efficiency of proBNP processing and, in turn, increased secretion of inactive proBNP (Figure 11D).

### Discussion

We were recently able to produce a highly sensitive and accurate immunoassay system selective for human proBNP.<sup>7</sup> Our system includes a capture antibody that is the same as the one used in the conventional BNP assay system and recognizes an epitope in the C-terminal regions of proBNP and mature BNP, and a signal antibody that recognizes an epitope in the N-terminal portion of proBNP. Although the epitopes of the signal antibodies differ between our assay and the

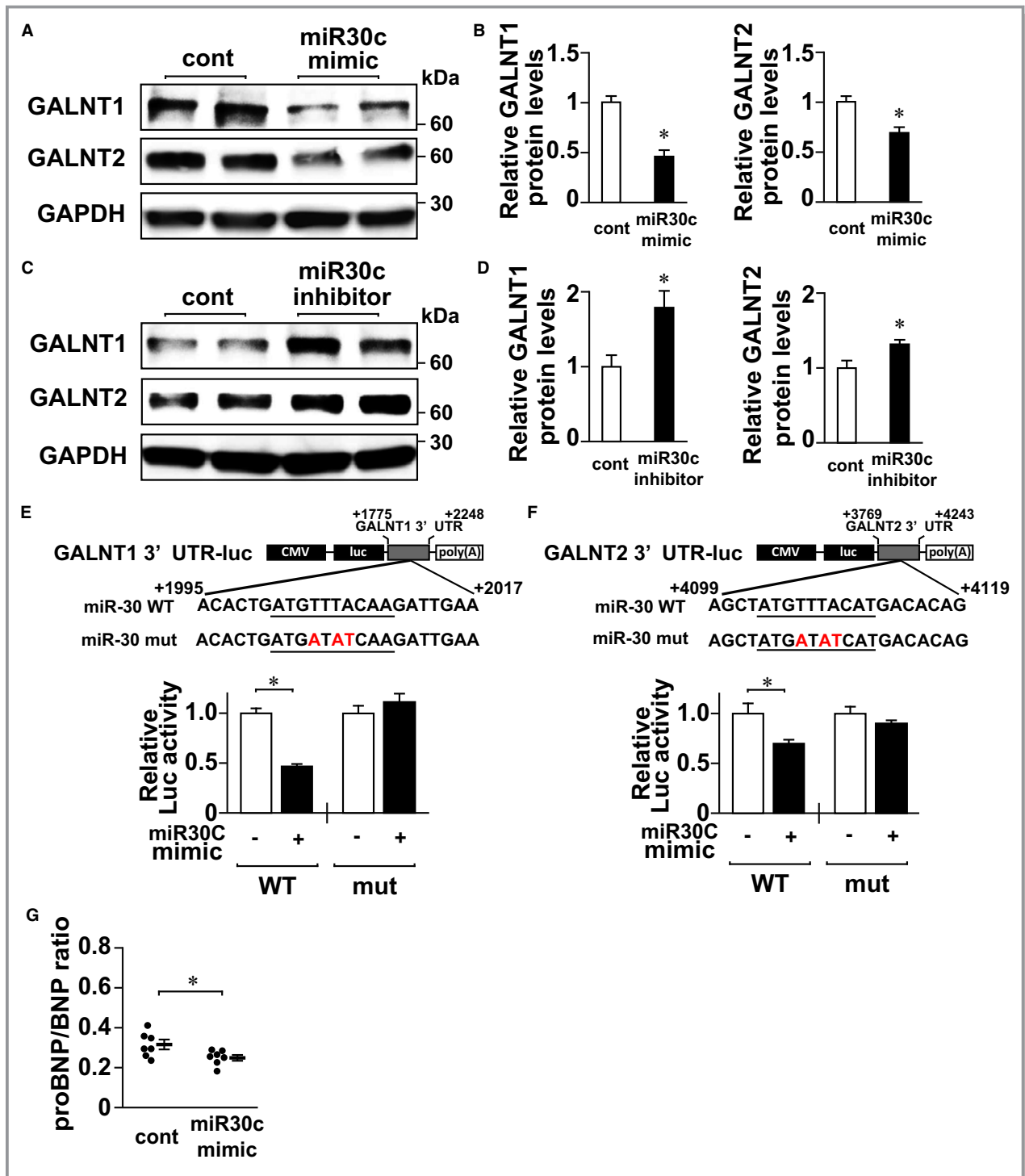


**Figure 9.** The microRNA-30 family regulates GALNT1/2 expression in cardiac myocytes. A through D, Expression of GALNT1/2 protein in neonatal rat ventricular myocytes (NRVMs) transfected with a miR-30c mimic (A and B) or a miR-30 inhibitor (C and D). Representative Western blots (A and C) and relative protein levels (n=6 per group) (B and D) are shown. The relative protein levels in untreated NRVMs (control) were assigned a value of 1.0. \* $P < 0.05$  vs control, using unpaired  $t$  test. E and F, Schema of wild-type (WT) and mut GALNT1 3'-untranslated region (3'UTR)-luc (upper panel of E) and WT and mut GALNT2 3'UTR-luc (upper panel of F), and relative luciferase activity of WT or mut GALNT1 3'UTR-luc (lower panel of E) and WT or mut GALNT2 3'UTR-luc (lower panel of F) with or without the miR-30 mimic. The relative luciferase activity of WT and mut GALNT1/2 3'UTR-luc without the miR-30 mimic was assigned a value of 1.0. \* $P < 0.05$  using unpaired  $t$  test within WT or mut GALNT1/2 3'UTR-luc group (n=8 each). Data are shown in means  $\pm$  SEM. G, prohormone for brain natriuretic peptide (proBNP)/BNP ratios in medium conditioned by NRVMs expressing WT-proBNP and transfected with a miR-30c mimic (n=7 each). Data are shown as dot plots with means  $\pm$  SEM. \* $P < 0.05$  using unpaired  $t$  test.



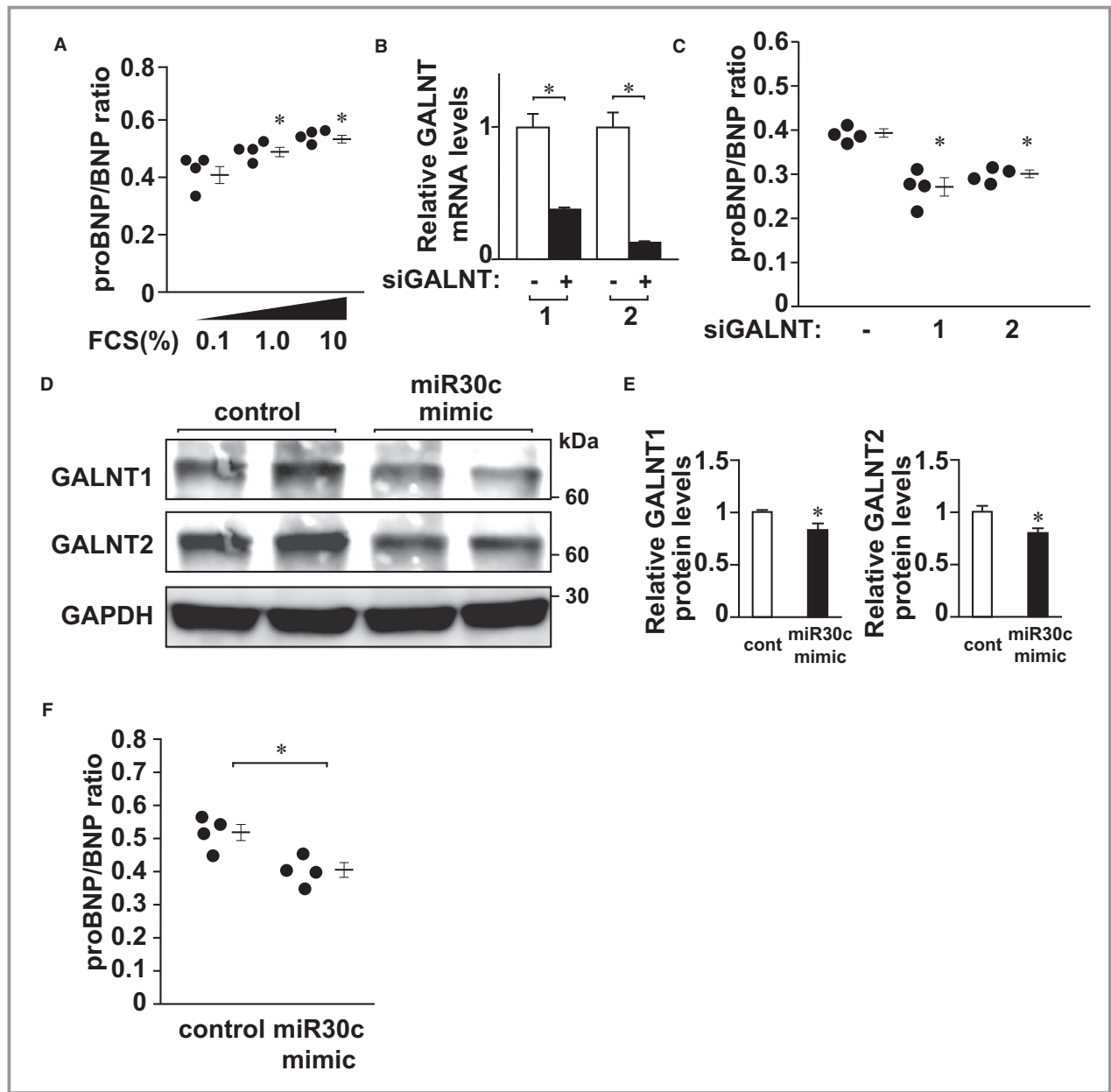


**Figure 10.** Mir-30-GALNT1/2 axis in human iPS-cardiomyocytes (CM) and mouse in vivo hearts. A, prohormone for brain natriuretic peptide (proBNP)/BNP ratios in medium conditioned by human iPS-CM stimulated with the indicated concentrations of fetal calf serum (FCS) (n=4 each). \**P*<0.05 vs 0.1% FCS using 1-way ANOVA with post hoc Fisher’s test. Data are shown as dot plots with means±SEM. B, mRNA expression of indicated GALNT genes in human iPS-CM transfected with the corresponding siRNAs. The mRNA levels in iPS-CM with control oligo were assigned a value of 1.0 (n=3 in each group). Data are shown as means±SEM. \**P*<0.05 vs control, using unpaired *t* tests. C, proBNP/BNP ratios in medium conditioned by human iPS-CM transfected with the corresponding siRNAs (n=4 each). \**P*<0.05 vs control oligo using 1-way ANOVA with post hoc Fisher’s test. Data are shown as dot plots with means±SEM. D and E, Expression of GALNT1/2 protein in human iPS-CM transfected with a miR-30c mimic. Representative Western blots (D) and relative protein levels (n=6 per group) (E) are shown. The relative protein levels in iPS-CM treated with control oligo (control) were assigned a value of 1.0. \**P*<0.05 vs control, using unpaired *t* test. F, proBNP/BNP ratios in medium conditioned by human iPS-CM transfected with a miR-30c mimic (n=4 each). Data are shown as dot plots with means±SEM. \**P*<0.05 using unpaired *t* test. G and H, Cardiac expression of GALNT1/2 protein in mice administered with a miR-30c inhibitor. Representative Western blots (G) and relative protein levels (n=5 per group) (H) are shown. We confirmed that in mice treated with rmiR-30c inhibitor the cardiac miR-30c expression levels were reduced to 4% of that in mice treated with negative control. The relative protein levels in mice treated with control scrambled oligo (control) were assigned a value of 1.0. \**P*<0.05 vs control, using unpaired *t* test.

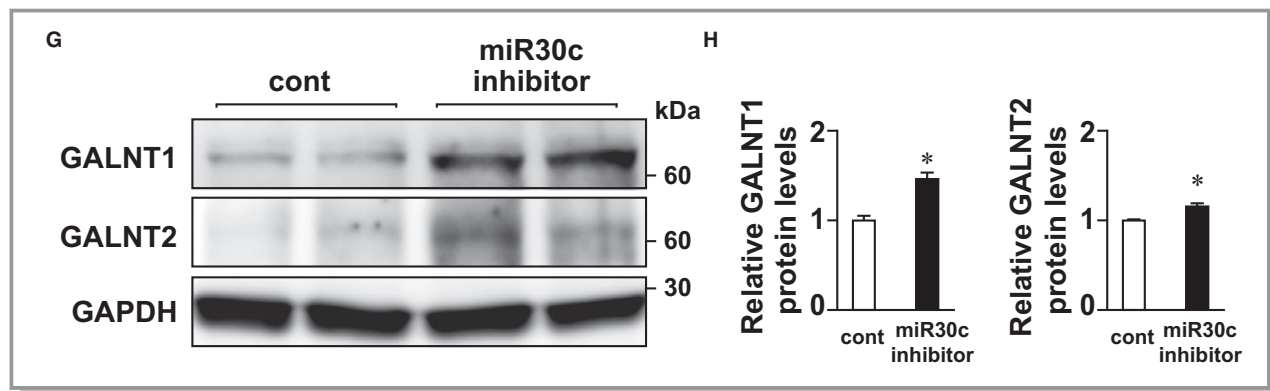


**Figure 10.** Continued

conventional one, their affinities for their epitopes are similar.<sup>7</sup> Consequently, by simultaneously using these 2 assay systems, we are able to calculate the proBNP/BNP ratio as an index of the proportion of proBNP among the immunoreactive BNP forms, which consists of proBNP and mature BNP. In this study, we showed that both the cardiac production of proBNP and the proportion of proBNP among secreted BNP forms increase with increases in the severity of heart failure in humans. Examination of peripheral metabolism revealed our results to be consistent with earlier studies showing that proBNP has much less ability to stimulate cGMP production than mature BNP.<sup>10</sup> It is therefore likely that the increased proportion of proBNP secreted from the heart attenuates the increase in cGMP levels, despite high plasma BNP levels in patients with severe heart failure.<sup>11,26,27</sup>

A recent study raised the possibility that proBNP is processed to mature BNP in the circulation.<sup>28</sup> Those investigators incubated histidine-tagged recombinant nonglycosylated-proBNP with venous serum and/or plasma collected from healthy subjects and used Western blot analysis to assess processing. In addition, Vodovar et al observed venous furin-like enzyme activity that was well correlated with NT-proBNP/total proBNP ratio and proposed that there may be peripheral processing of proBNP to mature BNP in acute heart failure patients.<sup>29</sup> By contrast, when we sampled venous blood from the superior vena cava or femoral vein and arterial blood from the cubital or femoral artery, respectively, of patients admitted for heart failure, we found that proBNP concentrations did not differ between a peripheral vein and artery in our population. This makes it unlikely that proBNP is metabolized in peripheral tissues or blood in these patients. The discrepancy between our results and those earlier findings may be explained in part by the differences between the in vivo and in vitro settings, between glycosylated proBNP and nonglycosylated proBNP, and/or between the clinical status of the heart failure patients.

We also clearly showed for the first time that, among human proBNP's 7 potential O-glycosylation sites, Thr71 and

Thr48 act cooperatively to inhibit proBNP processing and promote proBNP secretion by ventricular myocytes. Nevertheless, the proBNP secretion from myocytes expressing the T48/71glyco mutant, in which only T48 and T71 could be glycosylated, did not recapitulate the proBNP production from myocytes expressing WT-proBNP, suggesting that O-glycan attachments to the other 5 sites indirectly affect the processing of proBNP, probably by supporting the glycans attached to Thr48 and Thr71. Recent evidence indicates that GALNT-mediated O-glycosylation significantly affects protein processing, which can in turn modify pathophysiological processes.<sup>30</sup> For example, secretion of fibroblast growth factor-23 requires GALNT3-mediated O-glycosylation, which inhibits processing of fibroblast growth factor-23 into inactivated fragments.<sup>31,32</sup> In this study, we demonstrate that stress-induced increases in GALNT1/2 expression and the O-glycosylation they catalyze inhibits proBNP processing, leading to a higher proportion of inactive proBNP secretion under pathological conditions in the heart (Figure 11D). Though there is a report that GALNT3 can direct O-glycosylation at Thr71 in the synthetic proBNP peptide in vitro,<sup>33</sup> GALNT3 expression is reported to be barely detectable in the heart.<sup>24,30</sup> Furthermore, we confirmed that GALNT3 siRNA did not affect proBNP/BNP ratio in medium conditioned by NRVMs expressing WT-proBNP (Figure 7C and 7D).

The miR-30 family is ubiquitously expressed, but they are among the most highly expressed microRNAs in cardiac myocytes,<sup>25</sup> and recent in vitro observations revealed their involvement in the regulation of various cellular processes.<sup>34</sup> Cardiac expression of miR-30s reportedly decreases substantially over the course of pathological cardiac remodeling in both rodents and humans.<sup>25</sup> Consistent with that report, we found in the present study that levels of all members of the miR-30 family are significantly reduced in failing rat hearts and in hypertrophic NRVMs. It was recently reported that miR-30b and d negatively regulate GALNT1 and 7 expression in melanoma cells, and that silencing GALNT7 mediates miR-30d-inducible promigratory capacity in those cells.<sup>35</sup> This is

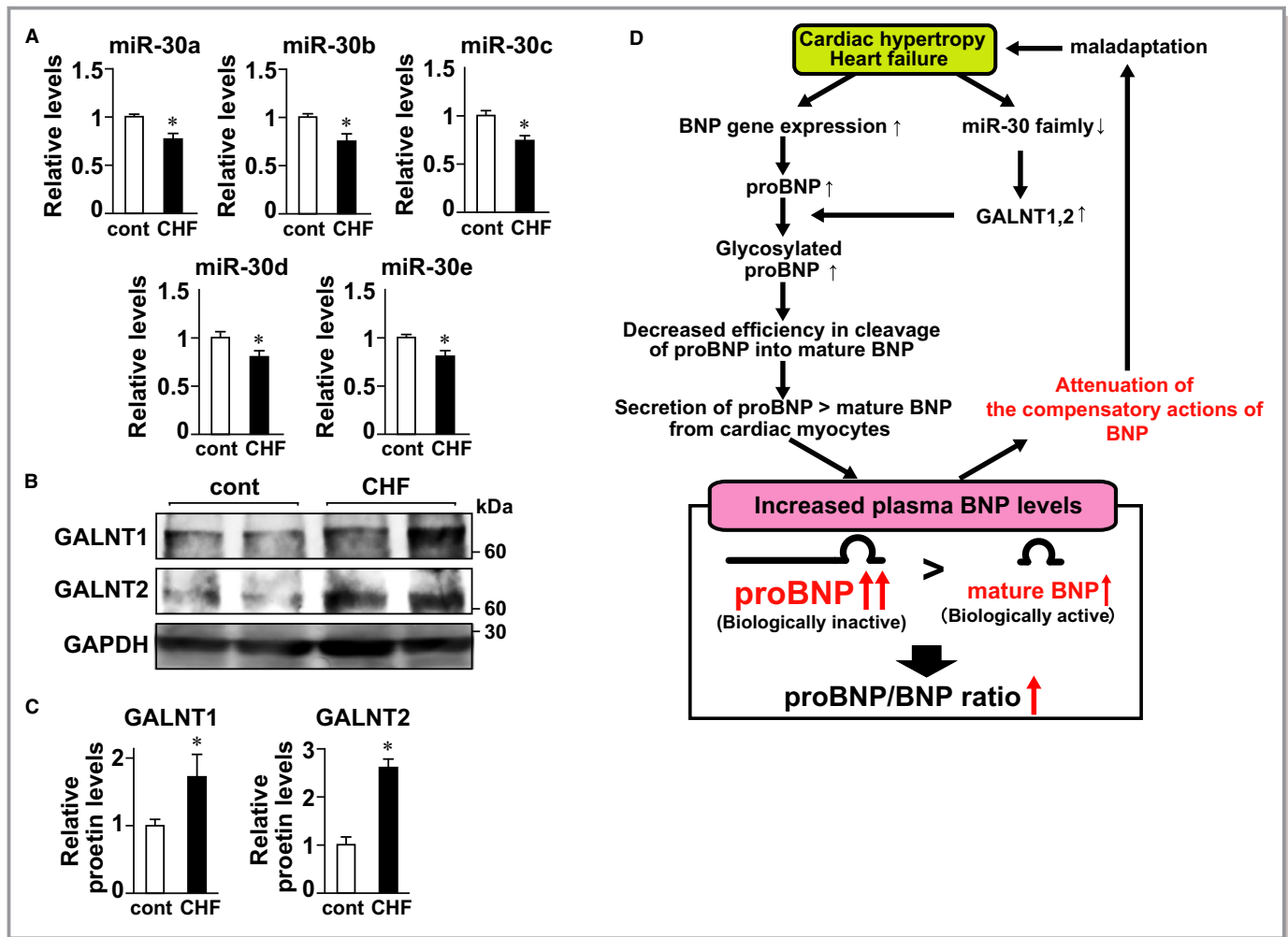


**Figure 11.** Expression of miR-30 family members is reduced and expression of GALNT 1/2 proteins is elevated in rat failing ventricles. A, Quantitative real-time polymerase chain reaction for miR-30 family members in ventricles from the healthy hearts of Dahl salt-sensitive (DS) rats fed a low-salt diet (cont) (n=17) and the failing hearts of DS rats fed a high-salt diet (CHF) (n=14). Rats in all groups were 17 weeks of age. Data are shown as means±SEM. The relative levels of miR-30s in normal hearts (cont) were assigned a value of 1.0. B and C, Expression of GALNT1/2 protein in ventricles from the normal hearts (cont) and the failing hearts (CHF) of DS rats. Representative Western blots (B) and relative protein levels (C) (n=6 per group) are shown. The relative protein levels in normal hearts (control) were assigned a value of 1.0. \*P<0.05 vs cont using unpaired t test. D, Proposed model of the miR-30s-GALNT axis-dependent regulation of glycosylation and secretion of unprocessed human prohormone for brain natriuretic peptide (proBNP). Under pathological conditions in the heart, BNP gene expression is increased, resulting in increased translation of proBNP. At the same time, reduction in miR-30 expression leads to increased GALNT1/2 expression, thereby increasing human proBNP glycosylation and decreasing the efficiency of proBNP processing to bioactive mature BNP. The resultant increase in the proportion of biologically inactive proBNP that is secreted attenuates the compensatory actions of BNP, despite its high plasma levels during the progression of heart failure.

consistent with our findings that miR-30-mediated suppression of GALNT1/2 expression decreases proBNP glycosylation and its secretion from cardiac myocytes.

Even relatively small changes in proBNP/BNP ratios, if it lasts for a long time, can sufficiently cause the decrease in the sum of cGMP production, thereby leading to the development or progression of cardiac diseases, because the potential of proBNP to produce cGMP is much weaker than that of mature BNP. In a recent clinical study, LCZ696, a neprilysin inhibitor combined with angiotensin receptor antagonist, significantly

repressed the cardiovascular events compared to enalapril, even though LCZ696 only slightly increased the plasma levels of BNP, demonstrating clearly that even small alterations in plasma levels of functional BNP can sufficiently affect the pathophysiological process of cardiovascular diseases.<sup>36</sup> Thus, the miR-30-GALNT pathway, which modulates the production and secretion of biologically active mature BNP, can be a novel therapeutic target for the treatment of heart failure. Further studies are needed to clarify the therapeutic implication of this pathway in humans.

**Table 5.** Morphometric Data, Heart Rates, and Blood Pressures in 17-Week-Old Dahl Salt-Sensitive Rats Fed a High-Salt Diet (CHF) or Low-Salt Diet (Control)

	Control (N=5)	CHF (N=8)	P Value
BW, g	429.5±5.8	357.5±12.8	0.001
HW/BW, mg/g	2.50±0.02	4.36±0.16	<0.001
LungW/BW, mg/g	3.73±0.18	6.05±0.52	0.057
TL, mm	58.0±0.7	57.1±0.0	0.241
HW/TL, mg/mm	1.89±0.1	2.71±0.5	<0.001
LungW/TL, mg/mm	2.79±1.3	3.76±3.2	0.041
HR, beat/min	413±18	467±20	0.089
SBP, mm Hg	118.8±3.1	193.5±6.3	<0.001

Unpaired *t* test was used for the analysis. *P*<0.05 is considered significant. BW indicates body weight; HR, heart rate; HW/BW, heart weight to body weight ratio; HW/TL, heart weight to tibia length ratio; LungW/BW, lung weight to body weight ratio; LungW/TL, lung weight to tibia length ratio; SBP, systolic blood pressure; TL, tibia length.

Our study has some limitations. First, the number of the samples in the human study 2 is relatively small. Second, we did not have patients' myocardium samples that enable us to evaluate cardiac miR-30 or GALNT1/2 expression levels in the patients enrolled in this study. Future studies examining the association between cardiac levels of miR-30 or GALNT1/2 and plasma proBNP/BNP ratios in human are needed.

In summary, our study sheds light on a novel molecular pathway leading to impairment of compensatory BNP actions that is mediated by a miR-30-GALNT1/2 axis during the development of heart failure in humans. Further investigation of the roles played by this pathway in the progression of heart failure could serve as the basis for novel therapeutic approaches to the prevention and treatment of chronic heart failure.

**Table 6.** Echocardiographic Parameters in 17-Week-Old Dahl Salt-Sensitive Rats Fed a High-Salt Diet (CHF) or Low-Salt Diet (Control)

	Control (N=14)	CHF (N=13)	P Value
HR, beats/min	441.9±10.7	473.0±30.3	0.410
IVS, mm	1.28±0.05	1.86±0.03	<0.001
PW, mm	1.49±0.10	1.96±0.01	0.012
LVDd, mm	7.85±0.10	7.37±0.22	0.053
LVDs, mm	3.00±0.07	4.22±0.26	<0.001
% FS, %	61.7±0.8	42.5±2.5	<0.001

Unpaired *t* test was used for the analysis. *P*<0.05 is considered significant. %FS indicates percent fractioning shortening of left ventricle; HR, heart rate; IVS, thickness of interventricular septum; LVDd, left ventricular end-diastolic diameter; LVDs, left ventricular end-systolic diameter; PW, thickness of left ventricular posterior wall.

## Acknowledgments

We thank Yukari Kubo and Mebae Kobayashi for their excellent secretarial work and Mizuho Takemura, Miku Ohya, Akiko Abe, and Inge van der Made for their excellent technical support.

## Sources of Funding

This research was supported by Grants-in-Aid for Scientific Research from the Japan Society for the Promotion of Science 23390210 and 24659386 (Koichiro Kuwahara), 24591095 (Kinoshita), 22590810 and 25461107 (Nakagawa), 25126712 and 23126511 (Nishikimi), and 21229013 (Kazuwa Nakao); by a grant from the Japanese Ministry of Health, Labor and Welfare (to Kazuwa Nakao); a grant from the Translational Research Network Program, Japan Agency for Medical Research and Development (AMED) (to Nakagawa); and by grants from the Japan Foundation for Applied Enzymology, the Takeda Science Foundation, the Hoh-ansha Foundation and the SENSHIN Medical Research Foundation (to Koichiro Kuwahara), and the Takeda Science Foundation (to Nakagawa). The assay kits used to measure human proBNP and BNP were kindly provided by Shionogi & Co. Ltd.

## Disclosures

The assay kits for measurement of human proBNP and BNP were provided to Yasuaki Nakagawa and Toshio Nishikimi by Shionogi & Co. Ltd. Hiroyuki Okamoto is an employee of Shionogi & Co. Ltd.

## References

- Sudoh T, Kangawa K, Minamino N, Matsuo H. A new natriuretic peptide in porcine brain. *Nature*. 1988;332:78–81.
- Yasue H, Yoshimura M, Sumida H, Kikuta K, Kugiyama K, Jougasaki M, Ogawa H, Okumura K, Mukoyama M, Nakao K. Localization and mechanism of secretion of B-type natriuretic peptide in comparison with those of A-type natriuretic peptide in normal subjects and patients with heart failure. *Circulation*. 1994;90:195–203.
- Kuwahara K, Saito Y, Takano M, Arai Y, Yasuno S, Nakagawa Y, Takahashi N, Adachi Y, Takemura G, Horie M, Miyamoto Y, Morisaki T, Kuratomi S, Noma A, Fujiwara H, Yoshimasa Y, Kinoshita H, Kawakami R, Kishimoto I, Nakanishi M, Usami S, Saito Y, Harada M, Nakao K. NRSF regulates the fetal cardiac gene program and maintains normal cardiac structure and function. *EMBO J*. 2003;22:6310–6321.
- Nishikimi T, Kuwahara K, Nakao K. Current biochemistry, molecular biology, and clinical relevance of natriuretic peptides. *J Cardiol*. 2011;57:131–140.
- Yancy CW, Jessup M, Bozkurt B, Butler J, Casey DE Jr, Drazner MH, Fonarow GC, Geraci SA, Horwich T, Januzzi JL, Johnson MR, Kasper EK, Levy WC, Masoudi FA, McBride PE, McMurray JJ, Mitchell JE, Peterson PN, Riegel B, Sam F, Stevenson LW, Tang WH, Tsai EJ, Wilkoff BL. 2013 ACCF/AHA guideline for the management of heart failure: executive summary: a report of the American College of Cardiology Foundation/American Heart Association Task Force on practice guidelines. *Circulation*. 2013;128:1810–1852.
- McMurray JJ, Adamopoulos S, Anker SD, Auricchio A, Bohm M, Dickstein K, Falk V, Filippatos G, Fonseca C, Gomez-Sanchez MA, Jaarsma T, Kober L, Lip GY, Maggioni AP, Parkhomenko A, Pieske BM, Popescu BA, Ronnevik PK, Rutten FH, Schwitler J, Seferovic P, Stepinska J, Trindade PT, Voors AA, Zannad F, Zeiger A; Guidelines ESCCFP. ESC guidelines for the diagnosis and treatment of acute and chronic heart failure 2012: the Task Force for the Diagnosis and Treatment of Acute and Chronic Heart Failure 2012 of the European Society of



Cardiology. Developed in collaboration with the Heart Failure Association (HFA) of the ESC. *Eur Heart J*. 2012;33:1787–1847.

7. Nishikimi T, Okamoto H, Nakamura M, Ogawa N, Horii K, Nagata K, Nakagawa Y, Kinoshita H, Yamada C, Nakao K, Minami T, Kuwabara Y, Kuwahara K, Masuda I, Kangawa K, Minamino N, Nakao K. Direct immunochemiluminescent assay for proBNP and total BNP in human plasma proBNP and total BNP levels in normal and heart failure. *PLoS One*. 2013;8:e53233.
8. Giuliani I, Rieunier F, Larue C, Delagneau JF, Granier C, Pau B, Ferriere M, Saussine M, Cristol JP, Dupuy AM, Merigeon E, Merle D, Villard S. Assay for measurement of intact B-type natriuretic peptide prohormone in blood. *Clin Chem*. 2006;52:1054–1061.
9. Nishikimi T, Kuwahara K, Nakagawa Y, Kangawa K, Minamino N, Nakao K. Complexity of molecular forms of B-type natriuretic peptide in heart failure. *Heart*. 2013;99:677–679.
10. Liang F, O'Rear J, Schellenberger U, Tai L, Lasecki M, Schreiner GF, Apple FS, Maisel AS, Pollitt NS, Protter AA. Evidence for functional heterogeneity of circulating B-type natriuretic peptide. *J Am Coll Cardiol*. 2007;49:1071–1078.
11. Tsutamoto T, Wada A, Maeda K, Hisanaga T, Maeda Y, Fukai D, Ohnishi M, Sugimoto Y, Kinoshita M. Attenuation of compensation of endogenous cardiac natriuretic peptide system in chronic heart failure: prognostic role of plasma brain natriuretic peptide concentration in patients with chronic symptomatic left ventricular dysfunction. *Circulation*. 1997;96:509–516.
12. Menon SG, Mills RM, Schellenberger U, Saqhir S, Protter AA. Clinical implications of defective B-type natriuretic peptide. *Clin Cardiol*. 2009;32:E36–E41.
13. Schellenberger U, O'Rear J, Guzzetta A, Jue RA, Protter AA, Pollitt NS. The precursor to B-type natriuretic peptide is an O-linked glycoprotein. *Arch Biochem Biophys*. 2006;451:160–166.
14. Semenov AG, Postnikov AB, Tamm NN, Seferian KR, Karpova NS, Bloschitsyna MN, Koshkina EV, Krasnoselsky MI, Serebryanaya DV, Katrukha AG. Processing of pro-brain natriuretic peptide is suppressed by O-glycosylation in the region close to the cleavage site. *Clin Chem*. 2009;55:489–498.
15. Peng J, Jiang J, Wang W, Qi X, Sun XL, Wu Q. Glycosylation and processing of pro-B-type natriuretic peptide in cardiomyocytes. *Biochem Biophys Res Commun*. 2011;411:593–598.
16. Nishikimi T, Nakagawa Y, Minamino N, Ikeda M, Tabei K, Fujishima A, Takayama K, Akimoto K, Yamada C, Nakao K, Minami T, Kuwabara Y, Kinoshita H, Tsutamoto T, Ishimitsu T, Kangawa K, Kuwahara K, Nakao K. Pro-B-type natriuretic peptide is cleaved intracellularly: impact of distance between O-glycosylation and cleavage sites. *Am J Physiol Regul Integr Comp Physiol*. 2015;309:R639–R649.
17. Inoko M, Kihara Y, Morii I, Fujiwara H, Sasayama S. Transition from compensatory hypertrophy to dilated, failing left ventricles in Dahl salt-sensitive rats. *Am J Physiol*. 1994;267:H2471–H2482.
18. Kato T, Niizuma S, Inuzuka Y, Kawashima T, Okuda J, Tamaki Y, Iwanaga Y, Narazaki M, Matsuda T, Soga T, Kita T, Kimura T, Shioi T. Analysis of metabolic remodeling in compensated left ventricular hypertrophy and heart failure. *Circ Heart Fail*. 2010;3:420–430.
19. Tijssen AJ, van der Made I, van den Hoogenhof MM, Wijnen WJ, van Deel ED, de Groot NE, Alekseev S, Fluiter K, Schroen B, Goumans MJ, van der Velden J, Duncker DJ, Pinto YM, Creemers EE. The microRNA-15 family inhibits the TGFbeta-pathway in the heart. *Cardiovasc Res*. 2014;104:61–71.
20. Tanada Y, Shioi T, Kato T, Kawamoto A, Okuda J, Kimura T. Branched-chain amino acids ameliorate heart failure with cardiac cachexia in rats. *Life Sci*. 2015;137:20–27.
21. Okita K, Matsumura Y, Sato Y, Okada A, Morizane A, Okamoto S, Hong H, Nakagawa M, Tanabe K, Tezuka K, Shibata T, Kunisada T, Takahashi M, Takahashi J, Saji H, Yamanaka S. A more efficient method to generate integration-free human iPS cells. *Nat Methods*. 2011;8:409–412.
22. Uosaki H, Fukushima H, Takeuchi A, Matsuoka S, Nakatsuji N, Yamanaka S, Yamashita JK. Efficient and scalable purification of cardiomyocytes from human embryonic and induced pluripotent stem cells by VCAM1 surface expression. *PLoS One*. 2011;6:e23657.
23. Masumoto H, Ikuno T, Takeda M, Fukushima H, Marui A, Katayama S, Shimizu T, Ikeda T, Okano T, Sakata R, Yamashita JK. Human iPS cell-engineered cardiac tissue sheets with cardiomyocytes and vascular cells for cardiac regeneration. *Sci Rep*. 2014;4:6716.
24. Bennett EP, Mandel U, Clausen H, Gerken TA, Fritz TA, Tabak LA. Control of mucin-type O-glycosylation: a classification of the polypeptide GalNAc-transferase gene family. *Glycobiology*. 2012;22:736–756.
25. Duisters RF, Tijssen AJ, Schroen B, Leenders JJ, Lentink V, van der Made I, Herias V, van Leeuwen RE, Schellings MW, Barenbrug P, Maessen JG, Heymans S, Pinto YM, Creemers EE. miR-133 and miR-30 regulate connective tissue growth factor: implications for a role of microRNAs in myocardial matrix remodeling. *Circ Res*. 2009;104:170–178, 6p following 178.
26. Dickey DM, Potter LR. ProBNP(1-108) is resistant to degradation and activates guanylyl cyclase-A with reduced potency. *Clin Chem*. 2011;57:1272–1278.
27. Heublein DM, Huntley BK, Boerrigter G, Cataliotti A, Sandberg SM, Redfield MM, Burnett JC Jr. Immunoreactivity and guanosine 3',5'-cyclic monophosphate activating actions of various molecular forms of human B-type natriuretic peptide. *Hypertension*. 2007;49:1114–1119.
28. Huntley BK, Sandberg SM, Heublein DM, Sangaralingham SJ, Burnett JC Jr, Ichiki T. Pro-B-type natriuretic peptide-1-108 processing and degradation in human heart failure. *Circ Heart Fail*. 2015;8:89–97.
29. Vodovar N, Seronde MF, Laribi S, Gayat E, Lassus J, Boukef R, Nouria S, Manivet P, Samuel JL, Logeart D, Ishihara S, Cohen Solal A, Januzzi JL Jr, Richards AM, Launay JM, Mebazaa A, Network G. Post-translational modifications enhance NT-proBNP and BNP production in acute decompensated heart failure. *Eur Heart J*. 2014;35:3434–3441.
30. Schjoldager KT, Clausen H. Site-specific protein O-glycosylation modulates proprotein processing—deciphering specific functions of the large polypeptide GalNAc-transferase gene family. *Biochim Biophys Acta*. 2012;1820:2079–2094.
31. Topaz O, Shurman DL, Bergman R, Indelman M, Ratajczak P, Mizrahi M, Khamaysi Z, Behar D, Petronius D, Friedman Y, Zelikovic I, Raimer S, Metzker A, Richard G, Sprecher E. Mutations in GALNT3, encoding a protein involved in O-linked glycosylation, cause familial tumoral calcinosis. *Nat Genet*. 2004;36:579–581.
32. Kato K, Jeanneau C, Tarp MA, Benet-Pages A, Lorenz-Depiereux B, Bennett EP, Mandel U, Strom TM, Clausen H. Polypeptide GalNAc-transferase T3 and familial tumoral calcinosis. Secretion of fibroblast growth factor 23 requires O-glycosylation. *J Biol Chem*. 2006;281:18370–18377.
33. Schjoldager KT, Vester-Christensen MB, Goth CK, Petersen TN, Brunak S, Bennett EP, Lavery SB, Clausen H. A systematic study of site-specific GalNAc-type O-glycosylation modulating proprotein convertase processing. *J Biol Chem*. 2011;286:40122–40132.
34. Pan W, Zhong Y, Cheng C, Liu B, Wang L, Li A, Xiong L, Liu S. MiR-30-regulated autophagy mediates angiotensin II-induced myocardial hypertrophy. *PLoS One*. 2013;8:e53950.
35. Gaziel-Sovran A, Segura MF, Di Micco R, Collins MK, Hanniford D, Vega-Saenz de Miera E, Rakus JF, Dankert JF, Shang S, Kerbel RS, Bhardwaj N, Shao Y, Darvishian F, Zavadil J, Erlebacher A, Mahal LK, Osman I, Hernandez E. miR-30b/30d regulation of GalNAc transferases enhances invasion and immunosuppression during metastasis. *Cancer Cell*. 2011;20:104–118.
36. Packer M, McMurray JJ, Desai AS, Gong J, Lefkowitz MP, Rizkala AR, Rouleau JL, Shi VC, Solomon SD, Swedberg K, Zile M, Andersen K, Arango JL, Arnold JM, Belohlavek J, Bohm M, Boytsov S, Burgess LJ, Cabrera W, Calvo C, Chen CH, Dukat A, Duarte YC, Erglis A, Fu M, Gomez E, Gonzalez-Medina A, Hagege AA, Huang J, Katova T, Kiatchoosakun S, Kim KS, Kozan O, Llamas EB, Martinez F, Merkely B, Mendoza I, Mosterd A, Negrusz-Kawecka M, Peuhkurinen K, Ramires FJ, Refsgaard J, Rosenthal A, Senni M, Sibulo AS Jr, Silva-Cardoso J, Squire IB, Starling RC, Teerlink JR, Vanhaecke J, Vinereanu D, Wong RC; Investigators P-H, Coordinators. Angiotensin receptor neprilysin inhibition compared with enalapril on the risk of clinical progression in surviving patients with heart failure. *Circulation*. 2015;131:54–61.

Downloaded from <http://jaha.ahajournals.org/> by guest on November 6, 2017

**MiR30–GALNT1/2 Axis–Mediated Glycosylation Contributes to the Increased Secretion of Inactive Human Prohormone for Brain Natriuretic Peptide (proBNP) From Failing Hearts**

Yasuaki Nakagawa, Toshio Nishikimi, Koichiro Kuwahara, Aoi Fujishima, Shogo Oka, Takayoshi Tsutamoto, Hideyuki Kinoshita, Kazuhiro Nakao, Kosai Cho, Hideaki Inazumi, Hiroyuki Okamoto, Motohiro Nishida, Takao Kato, Hiroyuki Fukushima, Jun K. Yamashita, Wino J. Wijnen, Esther E. Creemers, Kenji Kangawa, Naoto Minamino, Kazuwa Nakao and Takeshi Kimura

*J Am Heart Assoc.* 2017;6:e003601; originally published February 10, 2017;  
doi: 10.1161/JAHA.116.003601

The *Journal of the American Heart Association* is published by the American Heart Association, 7272 Greenville Avenue, Dallas, TX 75231  
Online ISSN: 2047-9980

The online version of this article, along with updated information and services, is located on the World Wide Web at:

<http://jaha.ahajournals.org/content/6/2/e003601>

Subscriptions, Permissions, and Reprints: The *Journal of the American Heart Association* is an online only Open Access publication. Visit the Journal at <http://jaha.ahajournals.org> for more information.